Performance Evaluation of Bismuth Telluride (Bi_2Te_3) Based Thermoelectric Generator : A Simulation Study

Kedir Hussien Kawo

A Thesis Submitted to the Department of Applied Physics
School of Applied Natural Science

Presented in Partial Fulfillment of the Requirement for Master's of Science in Applied Physics (Statistical Physics)

Office of Graduate Studies

Adama Science and Technology University

June, 2024

Adama, Ethiopia

Performance Evaluation of Bismuth Telluride (Bi_2Te_3) Based Thermoelectric Generator: A Simulation Study

Kedir Hussien Kawo

Major-Advisor: Kumneger Tadele (PhD)
Co-Advisor: Gashaw Beyene (PhD)

A Thesis Submitted to the Department of Applied Physics
School of Applied Natural Science

Presented in Partial Fulfillment of the Requirement for Master's of Science in Applied Physics (Statistical Physics)

Office of Graduate Studies

Adama Science and Technology University

June, 2024

Adama, Ethiopia

Declaration

I hereby declare that this Master Thesis entitled ***" Performance Evaluation of Bismuth Telluride (Bi_2Te_3) Based Thermoelectric Generator: A Simulation Study"*** is my original work. That is, it has not been submitted for the award of any academic degree, diploma or certificate in any other university. All sources of materials that are used for this thesis have been duly acknowledged through citation.

Name of Student	Signature	Date

Recommendation of Advisors

We, the advisors of this thesis, hereby certify that we have read the revised version of the thesis entitled ***" Performance Evaluation of Bismuth Telluride (Bi_2Te_3) Based Thermoelectric Generator: A Simulation Study "*** prepared under our guidance by **Kedir Hussien Kawo**. Submitted in partial fulfillment of the requirements for the degree of Master of Science in Applied Physics. Therefore, we recommend the submission of a revised version of the thesis to the department following the applicable procedures.

Major Advisor	Signature	Date
Co-advisor	Signature	Date

Approval Page

We, the advisors of the thesis entitled*" Performance Evaluation of Bismuth Telluride (Bi_2Te_3) Based Thermoelectric Generator: A Simulation Study"* and developed by **Kedir Hussien Kawo**, hereby certify that the recommendation and suggestions made by the board of examiners are appropriately incorporated into the final version of the thesis.

Major Advisor	Signature	Date
Co-advisor	Signature	Date

We, the undersigned, members of the Board of Examiners of the thesis by **Kedir Hussien Kawo** have read and evaluated the thesis entitled *" Performance Evaluation of Bismuth Telluride (Bi_2Te_3) Based Thermoelectric Generator: A Simulation Study"* and examined the candidate during open defense. This is, therefore, to certify that the thesis is accepted for partial fulfillment of the requirement of the degree of Master of Science in Physics.

Chairperson	Signature	Date
Internal Examiner	Signature	Date
External Examiner	Signature	Date

Final approval and acceptance of the thesis is contingent upon submission of its final copy to the Office of Postgraduate Studies (OPGS) through the Department Graduate Council (DGC) and School Graduate Committee (SGC)..

Department Head	Signature	Date
School Dean	Signature	Date
Office of Postgraduate Studies, Dean	Signature	Date

Acknowledgement

First and foremost, I would like to express my gratitude to "Almighty Allah" for providing me with the chance to pursue graduate studies as well as for always being there for me and never letting me down in difficult times. Next, I would like to express my sincere appreciation and gratitude to my Advisors Dr. Kumneger Tadele and Dr. Gashaw Beyene for their support, guidance, encouragement, and patience throughout this research period. I have special thanks to Tadesse Lemma (PhD candidate) for sharing his valuable experience and providing me with very important materials. Again, also I would like to thank my parents and other family members for their unwavering moral support, guidance, and encouragement during my academic career. Lastly, I would like to sincerely thank Adama Science and Technology University's School of Applied Natural Sciences, Department of Applied Physics program for providing me with a grant that allowed me to finish my studies.

Contents

List of Figures

List of Tables

List of Acronyms and Abbreviations

TE	Thermoelectric
σ	Electrical conductivity
κ	Thermal conductivity
κ_l	Lattice Thermal conductivity
κ_e	Electronic Thermal conductivity
κ_T	Total Thermal conductivity
S	Seebeck coefficient
ΔV	Voltage difference
ΔT	Change in temperature between the hot and cold sides
V	Voltage
I	current
A	cross-sectional area
T_H	hot side temperature
T_C	cold side temperature
ZT	dimensionless figure of merit
TAGS	Tellurium-Antimony-Germanium-Silver
BTE	Boltzmann Transport Equation
NEMD	Non-equilibrium molecular Dynamics
MD	molecular Dynamics
PV	photovoltaic
NSCF	Non self consistent field

Abstract

In this thesis, a detailed performance evaluation of a Bismuth telluride (Bi_2Te_3) based thermoelectric generator was conducted through simulation studies. Two computational methods were employed - non-equilibrium molecular dynamics (NEMD) and Boltzmann transport equation (BTE) to comprehensively determine the thermoelectric properties of Bi_2Te_3 over the temperature range of 100-800K. The NEMD method was used to calculate the lattice thermal conductivity, which was found to decrease with increasing temperature due to enhanced phonon scattering. The BTE method was then utilized to evaluate the electronic transport properties, including electronic thermal conductivity, electrical conductivity, and Seebeck coefficient. The results showed that electronic thermal conductivity increased with temperature as more charge carriers became thermally excited, while electrical conductivity decreased due to the dominant effect of phonon scattering at higher temperatures. The Seebeck coefficient was observed to rise with increasing temperature as the energy distribution of electrons broadened, allowing more charge carriers to participate in the thermoelectric process. By combining these calculated thermoelectric properties, the dimensionless figure of merit (ZT) was determined, and the efficiency of the Bi_2Te_3-based thermoelectric generator was estimated to be approximately 7.56% when the sink temperature was maintained at 300K and the source temperature was varied from 300-800K, in good agreement with literature report results.

Keywords: Bismuth telluride, non-equilibrium molecular dynamics, Boltzmann transport equation, Thermoelectric generator, Figure of merit

1. INTRODUCTION

1.1. Background of the study

Global emissions of greenhouse gases have increased as a result of rising power, heating, cooling, and air conditioning demands. To address the growing demand for energy, enormous efforts have been undertaken over the past few decades to investigate and develop alternative technologies. In this technologically driven society, green technologies like solar photovoltaic, wind turbines, hydrogenation, and biomass have begun to play a significant role in addressing energy and environmental challenges. These technologies have unquestionably benefited humanity because of their clean power generation method, which helps to mitigate various environmental difficulties. But it's impossible to overlook the greenhouse gas emissions produced during the production of these technologies, particularly when a lot of them are needed (Zheng et al., 2014).

As each of us knows, the world's total energy consumption has never stopped rising. The current green technology development and exploration efforts only shift the pressure from conventional power technologies to alternative technologies. The growing need for energy is one thing that hasn't altered. If we turned around, we would be overcome by the amount of resources being used (Zheng et al., 2014). It is ineffective and excessive. This raises questions about the root source of all connected global energy-related challenges that have been consuming a lot of our attention. The world is full of anxieties and anxiety, but the technologies themselves are not the source of these feelings. Rather, we are the ones who have been excessively and wastefully using our limited resources. We need to recognize the elegance in simplicity and re-evaluate the need for energy use in many contexts.

Recovering waste heat and increasing system efficiency are equally essential ways to improve energy efficiency. Only about 30% of the energy produced by fossil fuels is transformed into usable work, with the remainder of the energy being squandered as heat in internal combustion engine vehicles (Yan et al., 2020). The application of waste heat to thermoelectric generators for the production of electricity has long been a topic of interest in the field of energy recycling. Thermoelectric generators (TEGs) are solid-state devices that convert waste heat energy to electrical energy. Since waste heat is already free and readily available, using it as a heat source for thermoelectric generators (TEGs) is a cost-effective solution. It is estimated that over 70% of the world's energy production is lost to heat dispersion in the atmosphere, which is one of the main causes of global warming (Zevenhoven & Beyene, 2011). Thus, the use of thermoelectric generators (TEGs) to convert waste heat into electricity can help save energy and protect the environment. When compared to alternative power-generation methods, thermoelectric generator provide several advantages (Mamur & Ahiska, 2014). Because TEGs are environmentally friendly, scalable from small to huge heat sources, silent solid-state devices with no moving components, and incredibly reliable, they are marketed as attractive power-generation systems. Additionally, they have a longer lifespan and can produce electrical energy from low-grade thermal energy.

A Working the first mention of TEGs dates back to the early 1900s, when they were employed in radio systems fueled by gas (Telkes, 1947). To enable mobile radio operation, TEGs transformed the heat produced by burning gas into a DC power source for the radio. Low efficiency prevented TEGs from being commercialized since early TEGs were made of metal alloys, which are extremely inefficient thermoelectric materials (Rowe, 2018). Larger Seebeck coefficient semiconductor materials (Rowe, 2018) (on the order of $\pm 100 \mu V/K$) were used in the 1940s and 1950s as a result of advancements in semiconductor synthesis and fabrication. TEGs for waste heat energy recovery have been the subject of new research in the last three decades due to environmental laws, growing fossil fuel costs, and worries about climate change. The future of thermoelectric generators for solid-state cooling and direct thermal-electric energy conversion has improved due to recent developments in the engineering of thermoelectric materials with high figure of merit (Poudel et al., 2008). Widespread integration of TEGs into systems like factories, power plants, and cars where waste heat is a significant by-product is highly desired (Bell, 2008). Many firms, including Hyundai, GM (Thacher et al., 2007), BMW (Fairbanks, 2008), and Volkswagen (Očko et al., 2010), have designed cars with TEG fitted and enhanced fuel efficiency. When driving at highway speeds, BMW has recorded a 5% net increase in fuel efficiency for TEG-equipped vehicles (LaGrandeur et al., 2005). The integration of TEG modules on all current heavy trucks will be encouraged by the US Department of Energy, which has set an efficiency target of 10% (LaGrandeur et al., 2005). Car seats already have TEG coolers/heaters built in to enable more effective, localized cooling or heating. However, before TEGs are used in large-scale waste heat recovery systems, their efficiency must be significantly increased.

The current Thermoelectric generators (TEGs) used in waste heat recovery systems still face limitations in terms of conversion efficiency, impeding their widespread adoption for commercial purposes. In order to enhance TEG performance, researchers have identified two primary avenues of investigation. The first focuses on improving the thermoelectric efficiency of semiconductor materials used in TEGs, while the second involves optimizing the internal structure of TEGs. Thermoelectric materials are key components in thermoelectric devices, and the thermoelectric performance of these materials mostly determines the overall energy conversion efficiencies of the corresponding devices (Yang et al., 2022). The Seebeck effect, discovered by Thomas Seebeck around 200 years ago, enables thermoelectric materials to convert thermal energy into electricity. This conversion can be achieved using a compact solid-state semiconductor device, making thermoelectric materials highly attractive. Currently, the field of thermoelectrics is experiencing an exciting period, characterized by the discovery of new high-performance materials and innovative enhancement principles (Mori & Maignan, 2021). There is also significant progress in module development, bringing the long-held dream of widespread power generation applications closer to reality than ever before. Thermoelectric materials are increasingly important in two key areas (Bell, 2008). Firstly, they are crucial for energy-saving initiatives aimed at achieving recent goals of carbon neutrality and zero emissions. Secondly, they have a critical role in energy harvesting, providing dynamic power to the numerous sensors required for the future Internet of Things (IoT) society. Thermoelectric generators utilize pairs of n-type and p-type materials. In a study by Wenjie Xie *et al.*, it was demonstrated that scandium substitution in NbCoSn is effective in generating a high power factor for the p-type thermoelectric half Heusler, which serves as the weaker leg in thermoelectric pairs made from intermetallic materials (Yan et al., 2020).

The most commonly used thermoelectric material in commercial applications is Bi_2Te_3, which was discovered a long time ago but remains difficult to surpass interms of thermoelectric performance. Consequently, ongoing research focuses on improving its properties. One approach is to reduce the particle size, as this reduces thermal conductivity and increases the thermoelectric figure of merit. With this, a study by Cristina V.Manzano *et al.*, highlights the importance of the electrodeposition growth process in obtaining well-crystallized and oriented nanowires of Bi_2Te_3 . These nanowires exhibit a favorable aspect ratio and crystallographic orientation, which influence the mean free path of acoustic phonons and consequently result in lower thermal conductivity compared to bulk crystals of the same material (Manzano et al., 2019).

Lead telluride (PbTe) also demonstrates favorable thermoelectric properties when exposed to high temperatures. Its low thermal conductivity and significant Seebeck coefficient make it a promising material for applications requiring high temperatures. The addition of alloying elements like antimony (Sb) or selenium (Se) can further enhance its performance (Ding et al., 2018). Skutterudites, such as $CoSb_3$, and filled skutterudites like $(Co,Fe)Sb_3$ with guest atoms, have shown promising thermoelectric properties, particularly at elevated temperatures. These materials exhibit high ZT values due to their complex crystal structure and unique electrical properties. Silicides like Mg_2Si and $Ca_3Co_4O_9$ also exhibit excellent thermoelectric performance at high temperatures. Their crystalline structure and electrical characteristics contribute to their high energy conversion efficiency (Caballero-Calero et al., 2021). $TiNiSn$ and $ZrNiSn$ are notable examples of half-Heusler compounds that hold significant potential as thermoelectric materials, especially in high-temperature applications.. Given the significance of replacing fossil fuels in generating electricity, the current direction is to explore alternative energy sources. This involves focusing on the advancement of efficient thermoelectric materials, which have the capability to convert wasted heat from different sources into valuable electrical energy and vice versa (S. Huang & Xu, 2017). Thermoelectric materials, which can convert waste heat into electricity and vice versa, have garnered considerable interest due to their potential in addressing the global energy crisis. Although these materials have primarily been employed in specialized markets like small refrigerators, laser diode cooling devices, and automotive seat cooling, there have been numerous endeavors to expand their applications by improving their properties (Ryu et al., 2016). The performance of thermoelectric materials is assessed using a dimensionless figure of merit(zT),

$$zT = \frac{S^2\sigma}{\kappa}T \tag{1.1}$$

where T, S, σ, and κ are absolute temperature, Seebeck coefficient, electrical and total thermal conductivity, respectively (Heremans et al., 2008). Simultaneously attaining good electrical properties and minimizing thermal conductivity will lead to a high zT value. Thermoelectric conversion efficiency can be improved by maximizing the Seebeck coefficient, electrical conductivity, and lowering thermal conductivity. semiconductors that are used as thermoelectric materials can be grouped into three depending on the temperature range of the operation. These are Bismuth Telluride materials, Lead Telluride and Silicon-Germanium alloys. For a considerable time, bulk materials such as Bismuth telluride (Bi_2Te_3), antimony telluride (Sb_2Te_3), and their alloys have been recognized for their superior performance in terms of the figure of merit. This superiority is primarily attributed to their low lattice thermal conductivity at room temperature (C. Zhang et al., 2015). The theoretical approaches

commonly used to study phonon thermal conductivity include the Boltzmann transport equation (BTE), Monte Carlo simulations, and molecular dynamics (MD) simulations. The BTE and Monte Carlo methods rely on relaxation-time models to describe phonon scattering and often require fitting certain parameters to experimental data. In contrast, MD simulations do not require prior knowledge of phonon transport from experiments; instead, they use interatomic potentials as inputs. However, obtaining accurate interatomic potentials can be challenging, particularly for materials like Bi_2Te_3. Only recently, Huang *et al.* (B.-L. Huang & Kaviany, 2008) developed the first set of interatomic potentials for bulk crystals of Bi_2Te_3. These potentials were then used in Molecular dynamics simulations to predict phonon thermal conductivity. The results of their predictions showed good agreement with experimental data, even though the three-body potential forms used in the simulations were quite complex.

In recent decades, the ability to manufacture nanostructures with dimensions comparable to the mean free paths of phonons has enabled successful proof-of-concept demonstrations of high zT devices based on these materials. However, despite the long-standing importance of Bi_2Te_3 as a thermoelectric material, there have been limited modeling studies on thermal transport in its binary nanostructures. Pattamatta and Madnia researched the thermal transport properties of Bi_2Te_3-Sb_2Te_3 1D superlattices and 2D nanowire composites using the Boltzmann transport equation (BTE). They noted that the BTE approach utilized in their investigations relied on estimating phonon mean free paths through fitting to bulk thermal conductivities, which does not provide complete predictability. In contrast, molecular dynamics (MD) simulations have been effectively used to predict thermal transport in diverse bulk materials and nanoscale structures without the need for input fitting parameters. It depend only on suitable interatomic potentials and have demonstrated favorable agreement with experimental measurements of thermal transport in both bulk Bi_2Te_3 and its nanostructures (Termentzidis & Merabia, 2012).

Traditional thermoelectric materials typically exhibit a figure of merit (zT) of approximately 1 at room temperature (Hsu et al., 2004). Recently, the enhancement of zT with zT > 1 has been reported by many researchers. In a publication by Heremans *et al.* (Heremans et al., 2008), it was stated that Thallium-doped PbTe exhibited a zT value of 1.5 at a temperature of 773K. This enhancement was attributed to the local distortion of the density of states, which consequently improved the Seebeck coefficient. Additionally (Pei et al., 2011), reports a zT value of 1.8 at around 850K in Na-doped $PbTe_{1-x}Se_x$ alloys. This improvement was attributed to the convergence of multiple valleys in the valence bands. Numerous instances have reported improvements in the zT value of PbTe alloys (Ryu et al., 2016). Nevertheless, these advanced materials encounter various limitations concerning their environmental impact, economic feasibility, and technical viability. These limitations encompass the presence of toxic elements, elevated material costs, and inadequate zT values. To overcome these challenges and enable the exploration of novel thermoelectric materials with exceptional performance, computational simulations have emerged as invaluable tools. These simulations play a pivotal role in the discovery of new materials, guiding experimental endeavors, and offering insights into the obtained outcomes. For quite some time, researchers have been keen on employing computational simulations to model three fundamental properties: the Seebeck coefficient, electrical conductivity, and thermal conductivity.

1.2. Statement of the problem

The growing demand for energy to power our industrialized world and daily life applications has placed a significant strain on global energy supplies. Presently, a substantial portion, around 65%, of electrical power is generated through the combustion of non-renewable fossil fuels such as coal and petroleum. This heavy reliance on limited natural resources raises serious concerns about the long-term sustainability of our energy landscape. Estimates suggest that at the current rate of consumption, the available stocks of these non-renewable resources may be exhausted within the next 50 years (Gaurav & Pandey, 2017). Additionally, the thermal power plants responsible for around 70% of global electricity production operate at an efficiency of only 32%, meaning that a staggering 68% of the energy generated is lost as waste heat. Similar inefficiencies are observed in the automotive and steel manufacturing sectors, where substantial amounts of heat are discarded as a by-product of various industrial processes. In this context, the ability to extract useful energy from waste heat becomes a critical research area. Thermoelectric generators (TEGs) made of specialized thermoelectric materials (TEMs) offer a promising solution to this challenge. By utilizing the unique properties of these materials, TEGs have the potential to convert waste heat into practical electrical energy, thereby reducing our dependence on finite natural resources and improving the overall efficiency of energy utilization (LeBlanc, 2014). However, the effectiveness of TEGs is often limited by the low figure of merit (zT) of the constituent thermoelectric materials, which is a key parameter that quantifies their efficiency in the heat-to-electricity conversion process.

Despite advancements in the development of new thermoelectric materials with higher efficiency, enhancing the figure of merit (zT) remains a significant challenge. This challenge arises from the inherent trade-off between the electrical conductivity (σ) and thermal conductivity (κ) of these materials. Optimizing both properties simultaneously is crucial for achieving high thermoelectric performance, but it often proves to be a complex and intricate task. Certain materials, such as bismuth telluride (Bi_2Te_3) and its derivatives, have demonstrated promising figures of merit in the near room-temperature range, primarily due to their relatively low thermal conductivity. Investigating methods to further improve the figure of merit and optimize the efficiency of these materials, as well as developing corresponding thermoelectric devices with enhanced performance, is a critical research focus. By addressing this research problem, the study aims to contribute to the advancement of affordable and environmentally friendly energy solutions, particularly in the context of waste heat conversion and the mitigation of emissions associated with traditional power generation technologies. Overcoming the limitations of current thermoelectric materials and unlocking the full potential of waste heat recovery can lead to significant improvements in energy efficiency and sustainability, ultimately reducing our reliance on finite natural resources and mitigating the environmental impact of energy production.

1.3. Objectives

1.3.1 General Objective

The general objective of this study is to investigate the Efficiency of Bismuth telluride (Bi_2Te_3) based thermoelectric Generator.

1.3.2 Specific Objectives

The specific objectives of this study are:

- To investigate the temperature dependence of thermal conductivity of Bismuth telluride (Bi_2Te_3).
- To calculate the electrical conductivity of Bismuth telluride (Bi_2Te_3)
- To calculate seebeck coefficient of Bismuth telluride (Bi_2Te_3)
- To calculate the figure of merit of Bismuth Telluride (Bi_2Te_3).

1.4. Significance of the study

The study on Investigating the Performance of Bismuth Telluride Based Thermoelectric Generators holds significant importance for several reasons. Firstly, it advances thermoelectric technology as bismuth telluride is a well-known and widely used material in thermoelectric devices due to its excellent thermoelectric properties. Investigating the performance of a thermoelectric device based on bismuth telluride contributes to the advancement and understanding of thermoelectric technology. Secondly, this study can shed light on how effectively bismuth telluride-based thermoelectric devices can recover waste heat and generate electricity. Thermoelectric devices have the potential to harness waste heat energy and convert it into useful electrical energy, which has significant implications for energy harvesting, energy efficiency, and waste heat recovery in various industries and applications. Thirdly, as the world seeks sustainable and clean energy alternatives, thermoelectric devices offer a promising avenue. Investigating the performance of bismuth telluride-based thermoelectric devices contributes to the development of sustainable energy solutions. These devices can be employed in areas such as automotive, aerospace, industrial processes, and power generation to utilize waste heat and reduce greenhouse gas emissions.

Furthermore, the study of bismuth telluride-based thermoelectric devices involves materials research and engineering aspects, including understanding the properties and performance of bismuth telluride as a thermoelectric material. The findings from this study can provide valuable insights for researchers and engineers working on materials science, solid-state physics, and thermoelectric device development. Finally, bismuth telluride-based thermoelectric generators have a wide range of potential applications, including power generation in remote areas and waste heat recovery in industrial processes. Investigating their performance can contribute to the development and deployment of these technologies, leading to advancements in various industries and addressing energy-related challenges.

1.5. Scope and Limitations of the study

The scope of this study is to conduct a comprehensive performance evaluation of a bismuth telluride (Bi_2Te_3) based thermoelectric generator through detailed simulation and computational analysis. The key objectives of the study are to determine the crucial thermoelectric properties of Bi_2Te_3, including lattice thermal conductivity, electronic thermal conductivity, electrical conductivity, and Seebeck coefficient, over a wide temperature range of 100-800K. This is achieved through the utilization of two advanced computational techniques, non-equilibrium molecular dynamics (NEMD) and Boltzmann transport equation (BTE), which allow for the accurate calculation of these thermoelectric parameters. The study also aims to provide a thorough analysis of how temperature variations impact the performance of Bi_2Te_3, offering valuable insights into the material's behavior under different operating conditions. Building upon the obtained thermoelectric properties, the study calculates the dimensionless figure of merit (ZT) to assess the overall performance potential of Bi_2Te_3. Furthermore, the efficiency of the Bi_2Te_3-based thermoelectric generator is estimated under specified operating conditions, where the sink temperature is maintained at 300K and the source temperature is varied from 300-800K. The calculated efficiency is then compared with literature values reported for similar thermoelectric materials to validate the findings. Despite the comprehensive nature of the theoretical evaluation, the study is subject to several limitations. Firstly, the investigation is limited to a simulation-based approach and does not involve any experimental validation of the obtained results. Secondly, the efficiency calculation is based solely on the obtained ZT value and does not consider other practical factors, such as contact resistance, and manufacturing constraints, which can significantly impact the real-world performance of the thermoelectric generator. Additionally, the simulation study is confined to the temperature range of 100-800K, and the behavior of the Bi_2Te_3-based generator outside this range is not explored. Despite these limitations, the study presents a robust theoretical framework for evaluating the performance of Bi_2Te_3 based thermoelectric generators, laying the groundwork for future experimental investigations and practical implementation of thermoelectric technology.

1.6. Thesis Layout

This thesis entitled "Performance Evaluation of Bismuth telluride (Bi_2Te_3) Based Thermoelectric Generator: A Simulation Study", has five chapters: chapter 1, this chapter presents the background of the Thermoelectric generator in brief and it explains the introduction of thermoelectric materials, objectives, the problem statement, the significance, Scope, and Limitations of the study. Chapter 2, presents related literature reviews from previous studies that helped gain knowledge and understanding of the thesis better and discuss the energy conversion processes, theoretically predicting the efficiency of a thermoelectric generator. Chapter 3, focuses on the methodology utilized to achieve the objective of this thesis work. Chapter 4, presents the results and discussion of the major findings of this work. Chapter 5, summarizes the study, concludes with the overall study and it has recommendations.

2. LITERATURE REVIEW

2.1. An overview of energy harvesting

Energy harvesting refers to the practice of capturing and harnessing energy from readily available ambient sources in the surrounding environment. These ambient energy sources can include sunlight, wind, vibrations, thermal gradients, and electromagnetic radiation. It based on the idea that there are abundant sources of energy in our environment that can be converted into usable forms of power. This approach is particularly useful in situations where there is a match between the available energy and the energy requirements of a specific application or device (Enescu, 2019).

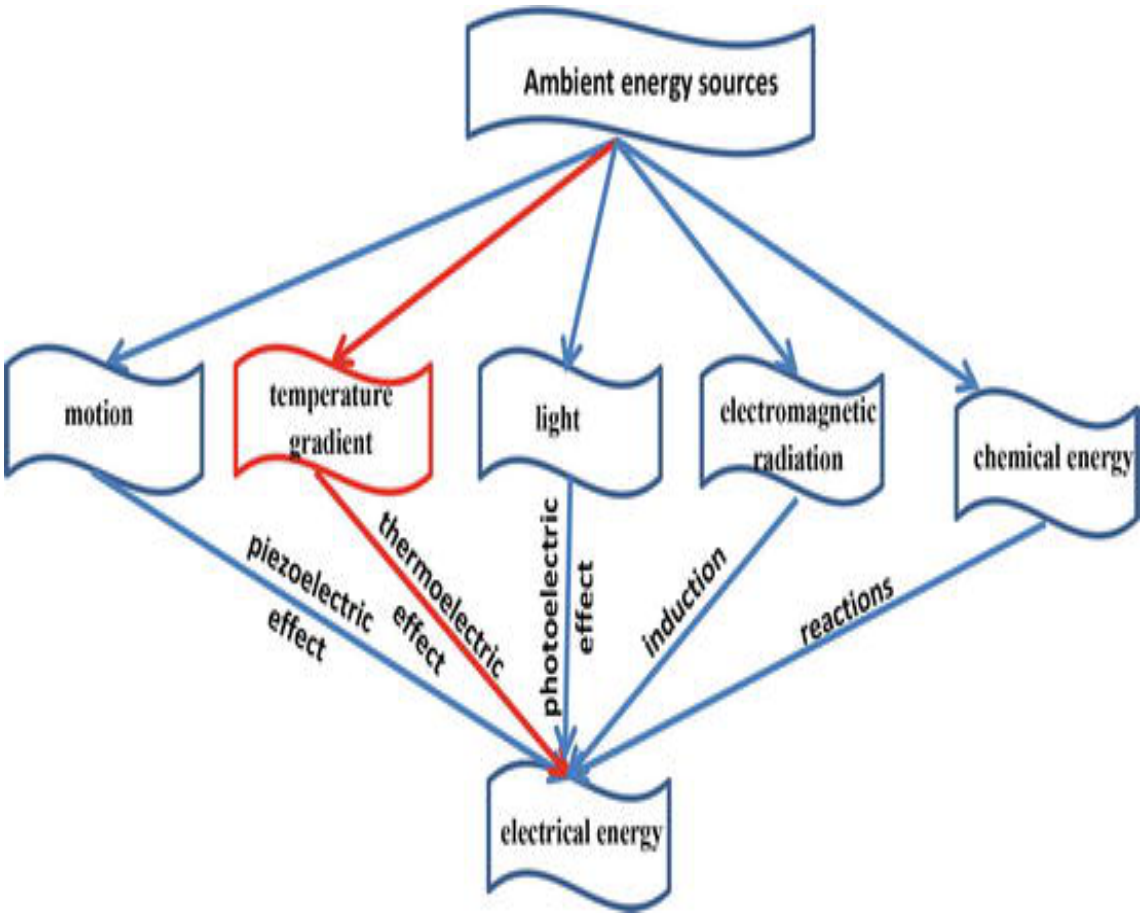

Figure 2.1: Sources of energy harvesting (Enescu, 2019).

An energy harvester consists of (Sim, 2012) an energy source, whether man-made or natural; one or more converters, which transform energy from the surroundings into electrical energy; and an energy storage device that preserves the captured energy. Energy harvesters find widespread use in various applications, and several types are commonly employed (Enescu, 2019). These include thermal harvesters, which utilize the thermoelectric effect to convert heat into electricity. Light harvesters operate on the photoelectric effect, converting light energy into electrical energy. Electromagnetic harvesters are based on induction principles, capturing and converting electromagnetic energy into usable electrical power.

Chemical harvesters rely on reactions occurring on electrode surfaces to generate electricity. Piezoelectric harvesters convert mechanical vibrations or human motion into electricity by harnessing the piezoelectric effect. Lastly, radio-frequency (RF) harvesters capture ambient radio-frequency radiation and convert it into electrical energy. These diverse energy harvesting technologies provide opportunities to harness various energy sources efficiently. Thermoelectric energy harvesting predominantly relies on the functioning of a thermoelectric generator (TEG).

The TEG directly converts heat into electrical energy by utilizing the Seebeck effect. This effect occurs when the movement of charge carriers, such as electrons and holes, within the TEG induces a temperature gradient across the device. Consequently, the TEG harnesses this temperature difference to generate electrical energy. The development of green energy technology has drawn the attention of experts in recent decades to reduce the usage of fossil fuels and greenhouse gas emissions. There are several benefits to using a thermoelectric harvester for energy gathering, including producing green energy, maintenance-free due to the usage of a small, incredibly dependable solid-state device; quiet and peaceful; excellent environmental efficiency due to the heat being extracted from waste heat sources and transformed into energy; operation at high temperatures; practical scalable solutions set up to gather relatively large amounts of energy as required (Snyder, 2009). Greenhouse gas emissions are decreased when energy is produced using a thermoelectric generator (TEG) instead of fossil fuels.

In contrast to conventional heat engines and thermodynamic PV systems, the TEG's energy conversion efficiency is just 5-15% (Cheng et al., 2011). The energy conversion efficiency is primarily affected by the temperature difference across the TEG system and the dimensionless thermoelectric figure-of-merit (ZT) (Camacho-Medina et al., 2014). When a TEG system is in operation, it is preferable to have the highest possible electric output power and efficiency. Only electric output power is important in waste heat recovery applications (Brownell & Hodes, 2014), and any heat that is not recovered is lost. Given that thermal energy harvesting has a low efficiency of 5–6%, this may provide a significant obstacle to its widespread use. The development of new thermoelectric materials has recently led to an increase in TEG efficiency of more than 10% (Shaikh & Zeadally, 2016). Figure 2.2 shows the process of recovering electrical energy from waste heat utilizing various sources.

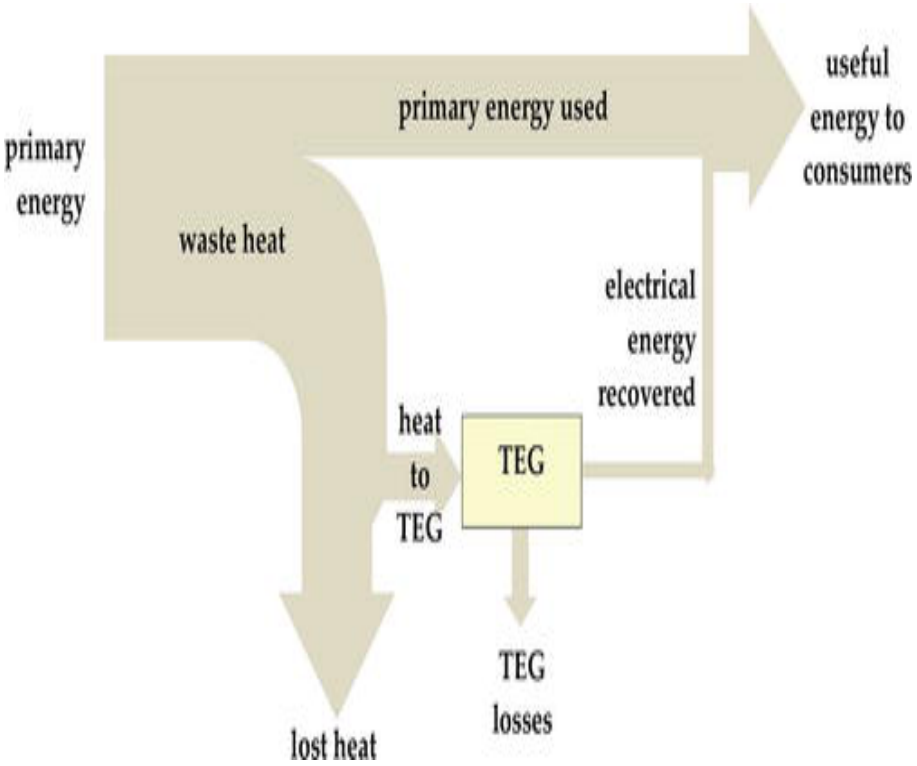

Figure 2.2: Recoverable electrical energy from waste heat (Enescu, 2019).

2.2. The significance and background of thermoelectric generating systems

TEGs are solid-state devices that convert thermal energy into electrical energy utilizing the thermoelectric effect (B. S. B. Singh, 2023). This phenomenon is explained by the Seebeck effect, which occurs when a temperature gradient is applied across incompatible semiconductor materials. Just two of the many applications where TEGs have recently achieved success are waste heat recovery and portable power generation. The ability of TEGs to recover heat that would otherwise be lost in a range of manufacturing and electricity-producing processes makes them beneficial (Umidbek Turg‘unboy o‘g et al., 2024). Vehicle and industrial machinery exhaust gasses are two typical examples of waste heat sources that leak into the environment and harm it. Through the capture and conversion of this waste heat into useful electrical energy, thermoelectric generators (TEGs) offer a viable solution for increasing energy efficiency and reducing greenhouse gas emissions. TEGs offer excellent dependability, compact size, and adaptability to a wide range of operating settings because they are solid-state devices with no moving parts. Their long service life, low maintenance requirements, and silent operation make them ideal for remote locations (Zebarjadi et al., 2012).

2.2.1 Thermoelectric Generator (TEG)

The thermoelectric generator (TEG) is a valuable device that directly converts thermal energy into electrical energy through the Seebeck effect. The behavior of TEG is determined by the interplay between Ohm’s law and Fourier’s law, which govern the properties of heat and electrical conductivity. In this regard, the TEG exhibits characteristics akin to a thermal engine that operates between two thermal sources (Juárez-Huerta et al., 2022). A thermoelectric generator (TEG) is composed of two legs made of thermoelectric materials (TEM) that

are electrically connected in series and thermally connected in parallel. Figure 2.3a illustrates the configuration of a thermoelectric generator (TEG) operating between two thermal reservoirs with temperatures T_h and T_c ($T_h \geq T_c$), with external thermal conductances K_h and K_c and internal resistance R of TEM with electric current I flowing through S, the Seebeck coefficient, and K, the thermal conductance of two arms of the couple in parallel, associated with the heat leak (open-circuit conductance) (Gonzalez-Hernandez & Arias-Hernandez, 2019). Figure 2.3b depicts a diagram illustrating the equivalent thermodynamic configurations for the thermoelectric generator (Ouerdane et al., 2015). The interaction between temperature and electric potential gradients gives rise to different thermoelectric effects (H. J. Goldsmid et al., 2010). As a result, the rates of heat input and heat rejection at the thermoelectric material (TEM) are given by

$$Q_h = IT_{eh}S + K(T_{eh} - T_{ec}) - \frac{RI^2}{2} \tag{2.1}$$

$$Q_h = IT_{ec}S + K(T_{eh} - T_{ec}) + \frac{RI^2}{2} \tag{2.2}$$

Where, the first term represents convective heat flow, with T_{eh} (T_{ec}) the effective temperature of TEM at the hot (cold) side (see Figure 2.3a). The second corresponds to a heat leak between the cold and hot sides, and the last term is the Joule heat received by each reservoir. For coupling with thermal sources, a Newtonian heat flow between a reservoir and TEM is assumed so that

$$Q_h = K_h(T_h - T_{eh}) \tag{2.3}$$

$$Q_c = K_c(T_{ec} - T_c) \tag{2.4}$$

The power output of the device is given by

$$P = Q_h - Q_c = IS(T_{eh} - T_{ec}) - I^2R \tag{2.5}$$

and the efficiency is given by

$$\eta = \frac{P}{Q_h} \tag{2.6}$$

2.2.2 Advantages of Thermoelectric generator

Thermoelectric generators have a variety of advantages that make them a compelling technology. Firstly, they offer direct energy conversion, unlike many heat engines that first convert thermal energy into mechanical energy and then convert this mechanical energy into electricity using an alternator. This direct conversion process is a key advantage of thermoelectric generators. Another significant advantage is the absence of moving parts and working fluids inside the thermoelectric generator. This results in low maintenance requirements and no additional costs associated with such components. The lack of moving parts also contributes to the long lifespan of thermoelectric generators, especially when working with constant heat sources. Thermoelectric generators are also unique in their ability to be scaled to different power requirements. They can be used for micro-generation in very limited spaces or to produce kilowatts of power, with no scale effect limiting their applications. This versatility makes them well-suited for a wide range of embedded systems and applications. Furthermore, thermoelectric generators operate in a noiseless manner, which is an important consideration for many applications where noise reduction is crucial. Additionally, any working position is possible for these generators, further enhancing their suitability for embedded systems and other specialized uses.

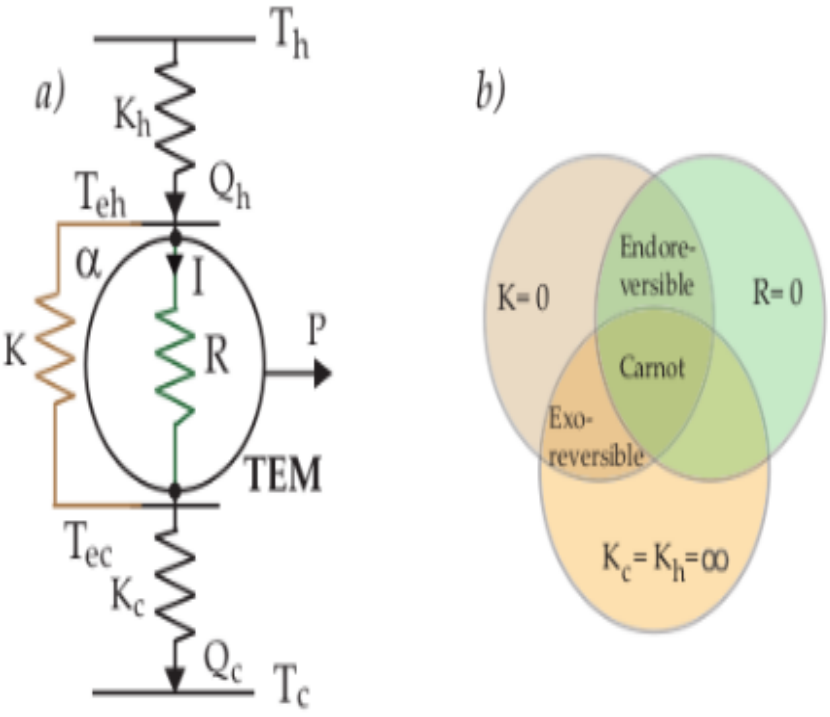

Figure 2.3: (a) The TEG's internal and external irreversibilities scheme. (b) Diagram illustrating thermodynamic configurations (Juárez-Huerta et al., 2022).

2.3. Factors affecting thermoelectric generator performance

Numerous factors can affect how well a thermoelectric generator (TEG) performs. Optimizing these factors can lead to an increase in a thermoelectric generator's efficiency and power production capacity.

2.3.1 The Effect of temperature gradient

The temperature gradient refers to the difference in temperature between the hot and cold sides of a thermoelectric generator (TEG). The power output of a TEG is directly influenced by this temperature gradient. When there is a larger temperature difference between the hot and cold sides of the TEG, more power can be generated. The TEG is capable of converting heat flux from the hotter region to the cooler region into electrical energy. A higher heat flow resulting from a larger temperature differential can lead to an increased power output of the TEG. This increase in temperature across the TEG also corresponds to a higher maximum power output (B. Singh et al., 2017). The voltage output of a TEG is also affected by the temperature gradient. The TEG operates based on the Seebeck effect, which produces an electric potential across the TEG when there is a temperature gradient. A larger temperature gradient results in a higher voltage output. Therefore, a TEG can generate more electrical power when there is a greater temperature differential (Tundee et al., 2014).

2.3.2 The effects of a system's heat source temperature

The temperature of the heat source has a significant impact on the performance of a thermoelectric generator (TEG). It is a crucial parameter that directly affects the power generation capability of the TEG. The power generation of the TEG is influenced by the tem-

perature gradient between its hot and cold sides. When the temperature of the heat source is increased, it results in a larger temperature gradient, leading to a greater temperature difference and consequently, an increased power output. Therefore, raising the temperature of the heat source has the potential to enhance the power output of the TEG. Thus, it can be said that using a heat collector with a high absorptivity and low emissivity in conjunction with a high input energy produces favorable results in terms of producing a thermoelectric generator that performs better (Cai et al., 2011).

2.3.3 The effect of load resistance

The power output and efficiency of a thermoelectric generator (TEG) system are significantly influenced by the load resistance. The voltage and current produced by the TEG depend on the load resistance. According to Ohm's law (V = IR), there is a direct relationship between the voltage across the load resistance, the current flowing through it, and the value of the load resistance itself. By selecting different load resistance values, it is possible to adjust the voltage and current levels to meet the specific requirements of an application. In a liquid-to-liquid generator, a study was conducted to determine the optimal electrical load resistance that maximizes thermoelectric generation (Lesage & Pagé-Potvin, 2013).

2.4. Thermoelectrics As Heat Engines

Thermoelectric devices function as solid-state heat engines. In contrast to conventional air conditioners that utilize two-phase fluids like R-134A as refrigerants, TE devices utilize electrons as their working fluid. The performance of TE devices is governed by several principal effects, as illustrated in Figure 2.4. In 1834, Peltier made an observation that applying a current across a junction made of dissimilar electrically conductive materials can result in either heating or cooling at the junction. When the current is reversed, the opposite effect occurs. Figure 2.4A illustrates why this phenomenon takes place. In materials such as semiconductors, metals, or semimetals, electric current is carried by electrons in n-type materials and by holes (which travel in the opposite direction) in p-type materials. When a voltage is applied in the correct direction across a p-n junction, electron-hole pairs are generated near the junction. Electrons move away from the junction in the n-type material, while holes move away in the p-type material. This process extracts energy from the junction area, causing it to cool down. On the other side, electrons and holes flow towards junctions where the pairs recombine, releasing energy and heating those junctions. At the bottom of Figure 2.4, a typical TE module is shown, designed in a way that all junctions on one side heat up while those on the other side cool down (Bell, 2008).

In 1821, Seebeck made an important observation that when dissimilar metals are connected in series electrically and in parallel thermally, and exposed to a temperature gradient, the needle of a magnet is deflected. This discovery forms the basis for thermoelectric (TE) power generation. As depicted in Figure 2.4B, if the junctions at the top are heated while those at the bottom are cooled, resulting in a temperature difference, electron-hole pairs are created at the hot end and absorb heat in the process. These pairs recombine and release heat at the cold ends. The temperature difference between the hot and cold ends of the TE elements generates a voltage potential known as the Seebeck voltage, which drives the flow of holes and electrons. This voltage appears across the bottom of the TE element legs (Bell, 2008). The Seebeck effect is also fundamental to the operation of thermocouples used extensively in temperature measurement systems. By making electrical connections from the

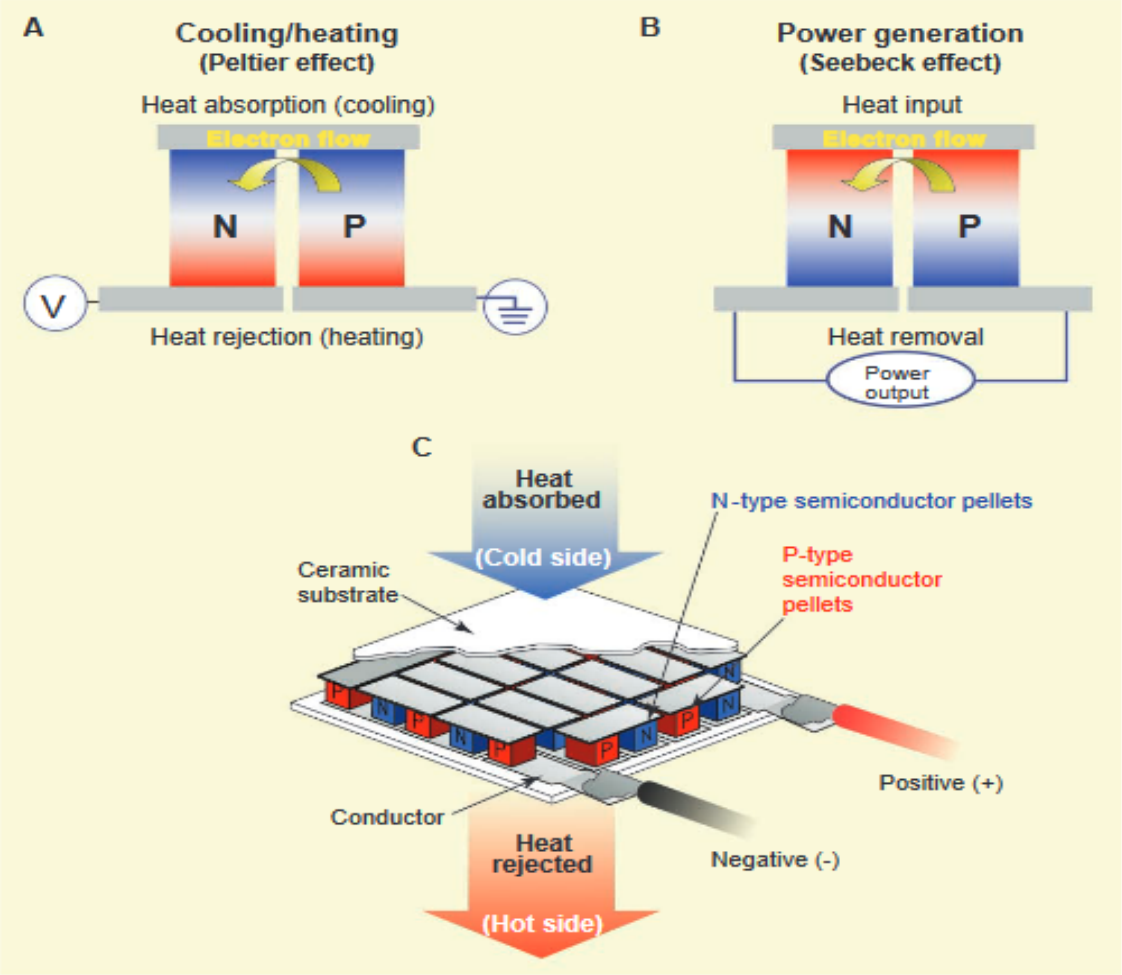

Figure 2.4: TE heat engines operate based on three primary effects. (A) when an electric current is passed through a TE junction, it either heats or cools due to the Peltier effect, depending on the direction of the current flow. (B) when there is a flow of heat across the junction, it generates an electrical current through the Seebeck effect. (C) practical TE generators maximize their performance by connecting numerous junctions in series, which increases the operating voltage and spreads the heat flow (Bell, 2008).

TE elements to an external load, power can be extracted. For this process to be efficient, it is crucial to identify materials that are good electrical conductors to minimize electron scattering and heat generation. Additionally, the materials should have low thermal conductivity to prevent significant heat backflow caused by the temperature difference between the hot and cold sides. Moreover, maximizing the Seebeck effect is important. However, optimizing these three parameters poses challenges as they are influenced by the electronic properties of the materials. Since the working fluid (electrons) conducts both electric current and unwanted heat, and the Seebeck effect diminishes with increasing electrical conductivity, it becomes necessary to simultaneously optimize these properties (Bell, 2008).

2.5. Efficiency evaluation of a Thermoelectric generator

Thermoelectric generators (TEGs), which are constructed of thermoelectric materials, are the greatest option for obtaining energy from waste heat. The thermoelectric conversion efficiency of Thermoelectric generator, is defined as the ratio of the electric output power

(P) delivered to the load to the rate of heat input (Q_h) absorbed at the hot junction of the TEG and transferred through it. In other words, the TEG converts the rate of heat input into electric output power (P) with an efficiency (η) (Enescu, 2019).

$$\eta = \frac{P}{Q_h} \tag{2.7}$$

The maximum efficiency of a thermoelectric generator (TEG) utilizing thermoelectric materials involves a parameter associated with the materials used (Sherman et al., 1960). This parameter is defined as,

$$\eta_{max} = \frac{T_h - T_c}{T_h} \frac{\sqrt{1+ZT}-1}{\sqrt{1+ZT}+\frac{T_c}{T_h}} \tag{2.8}$$

Where $T = \frac{T_h+T_c}{2}$, T_h and T_c are source and sink temperature, respectively. Z is called a figure of merit of the material used.

2.6. Thermoelectric effects

The thermoelectric effects are reversible phenomena that enable the direct conversion between thermal and electrical energy (Brownell & Hodes, 2014). Direct energy conversion is dependent on the physical transport properties of thermoelectric materials, such as thermal conductivity, electrical conductivity, and Seebeck coefficient. Additionally, their energy conversion efficiency is assessed based on the figure-of-merit (X. Zhang & Zhao, 2015). These materials possess the capability to convert thermal energy into electrical energy and vice versa. The primary phenomena involved in a thermoelectric device are the thermoelectric effects (Seebeck, Peltier, Thomson and the Joule effect). The Peltier effect occurs when electrical energy is converted into thermal energy and finds applications in cooling and heating. The corresponding device utilized in such applications is known as a thermoelectric cooler(TEC) (Enescu, 2019), which functions as an efficient temperature controller through thermoelectric modules. On the other hand, the Seebeck effect occurs when thermal energy is converted into electrical energy and is employed for power generation. The device used in such applications is referred to as a thermoelectric generator(TEG) (Champier et al., 2010).

2.7. Materials properties that affect efficiency and output power of a thermoelectric system.

The Seebeck coefficient, also known as thermopower, is commonly used to measure the voltage generated by a material in response to a temperature gradient. A higher Seebeck coefficient leads to a greater voltage output, which can potentially improve the power output of a thermoelectric generator (TEG). The electrical conductivity of a thermoelectric material also plays a significant role in the flow of electric current through the TEG. Increased electrical conductivity allows for enhanced electrical conduction and reduced electrical resistance, thereby leading to higher power generation (Xiao et al., 2012).

Furthermore, the thermal conductivity of a thermoelectric material plays a crucial role in its heat transfer efficiency. To improve the thermoelectric efficiency and maintain a larger temperature gradient across the thermoelectric generator (TEG), the material needs to have a lower thermal conductivity. By using materials with reduced thermal conductivity, excessive heat transfer can be mitigated, allowing for a higher temperature gradient that enhances

power generation. It is also important to consider the figure of merit (ZT), which is a dimensionless parameter that incorporates the Seebeck coefficient, electrical conductivity, and thermal conductivity of a material. A high ZT value indicates strong thermoelectric performance. In thermoelectric generators (TEGs), materials with higher ZT values generally exhibit improved efficiency and power generation capabilities (Caballero-Calero et al., 2021).

2.8. The dimensionless thermoelectric figure of merit (zT)

The dimensionless thermoelectric figure of merit zT is used to characterize a thermoelectric material performance, as well as the efficiencies of various TEGs (Snyder & Snyder, 2017). The figure of merit of thermoelectric materials is given by

$$zT = \frac{S^2\sigma}{\kappa}T = \frac{S^2\sigma}{\kappa_e + \kappa_l}T \tag{2.9}$$

where T , S, σ, κ_e and κ_l are absolute temperature, Seebeck coefficient or thermopower, electrical conductivity, electron thermal conductivity and lattice thermal conductivity respectively. The thermal conductivity has two contributions, one from the electrical carriers κ_e and the other from lattice vibrations κ_l. Electronic thermal conductivity is the thermal conductivity from electrons and holes transporting heat and lattice thermal conductivity originates from phonons traveling through the lattice. Indeed, the ZT value is a critical indicator of the thermoelectric properties of a material, with higher values indicating better performance. However, achieving significant improvements in the thermoelectric figure of merit has been challenging due to the complex relationship between the Seebeck coefficient, electrical conductivity, and thermal conductivity (Snyder & Toberer, 2008). Therefore, our primary objective to be enhancing the electrical transmission performance ($S^2\sigma$) of the material while reducing its heat transmission performance (κ) through the coordinated regulation of electrical and heat transmission.

According to the Wiedemann-Franz law, $\kappa_e = L\sigma T$, where L represents the Lorentz constant. This equation demonstrates a positive correlation between the electronic thermal conductivity and electrical conductivity. Thus, by reducing the thermal conductivity of the lattice, which has a weaker correlation, we can effectively optimize the thermoelectric figure of merit (Biswas et al., 2012). The ZT statistical results of a few common TE materials from recent years are summarized in Figure 2.5 Sun et al. (2022).

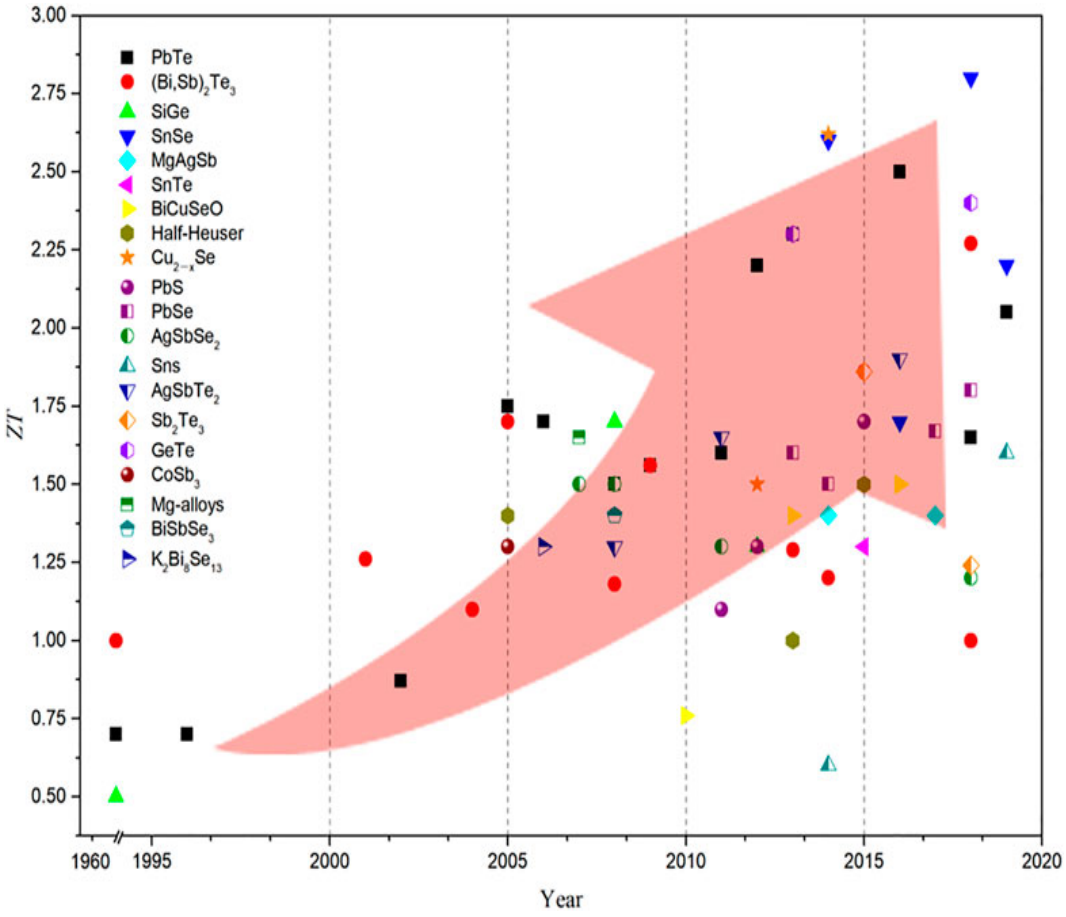

Figure 2.5: A few common thermoelectric materials Figure of merits in recent years (Sun et al., 2022)

.

2.9. Molecular Dynamics

Molecular dynamics (MD) is a computer simulation method that involves integrating the equation of motion of a group of interacting particles to track their temporal evolution. The method has provided significant insight into the behavior of interacting classical many-particle systems and has been applied to systems with several hundred to millions of particles. By employing a description of the interatomic interaction to numerically solve Newton's equation of motion, scientists can examine the physical movements of atoms and molecules. Utilizing the theoretical framework established by statistical mechanics, equilibrium and transport characteristics are determined (Badar et al., 2022). MD is a simulation method based on the numerical integration of Newton's equation of motion:

$$m_i \frac{d^2 r_i}{dt^2} = -\frac{\partial V_i}{\partial r_i} \tag{2.10}$$

where: m_i ,r_i and V_i denote respectively the mass of the particle i, its position vector and the inter-atomic potential. Solving the differential equations of motion (Eq. (2.10)) of a system of molecules that interact with one another via an intermolecular potential is the fundamental goal of the MD algorithm. Since the forces taken into account are typically conservative, they can be computed using equation (2.10). Because every molecule in the system interacts with every other molecule, there is a lot of computing involved (Steinhauser, 2012). As a

result, the simulation needs to perform a significant number of computationally demanding force field computations. The intermolecular potential model's precision and the numerical integrator's accuracy in solving the equations of motion are the main variables influencing the simulation's accuracy. The adaptability and flexibility in selecting the atomic potential is what makes MD so strong. In general, the entire potential can be broken down into the sum of

$$V(r_i) = \sum_i V_1(r_i) + \sum_{i<j} V_2(r_i, r_j) + \sum_{i<j<k} V_3(r_i, r_j, r_k) \tag{2.11}$$

where the first term accounts for the contribution from external fields, such as an electric field, acting on the individual particles. The second and third terms represent the two-body and three-body inter-atomic potentials, capturing the pairwise and three-particle interactions, respectively. The choice of the specific inter-atomic potential depends on the problem at hand (the type of atomic structure and the properties to be studied) as well as the need to accurately model a real system or an experimental setup. One of the simplest potentials used is the Lennard-Jones potential, where the total potential can be expressed as a sum of pair potentials between individual particles.:

$$V = \sum_{i<j} V_2(r_{ij}) \tag{2.12}$$

With

$$V_2(r_{ij}) = 4\varepsilon((\frac{\sigma}{r_{ij}})^{12} - (\frac{\sigma}{r_{ij}})^6) \tag{2.13}$$

This is the LJ pair potential, which depends only on the distance between neighbouring particles $r_{ij} = r_{ji}$. The interaction energy ε identifies with the depth well of the potential, and σ is the atomic diameter.

The integration scheme commonly used in MD is the Verlet algorithm which predicts the positions at time t + dt given the positions at the earlier times t and t - dt :

2.9.1 The Verlet algorithm

Loup Verlet introduced a molecular simulation algorithm based on central differences in 1967 (Verlet, 1967). The simple algorithm introduced by Loup Verlet in 1967 has proven to be highly effective in many cases of molecular dynamics (MD) simulations and is widely utilized. The algorithm can be derived by performing a Taylor expansion of the position coordinate in both forward and backward directions in time,

$$r(t + \Delta t) = r(t) + v(t)\Delta t + \frac{1}{2}a(t)\Delta t^2 + ... \tag{2.14}$$

$$r(t - \Delta t) = r(t) - v(t)\Delta t + \frac{1}{2}a(t)\Delta t^2 - ... \tag{2.15}$$

where, $v = \frac{dr}{dt}$, $a = \frac{d^2r}{dt^2} = \frac{F}{m}$ and Δt is the time step in the numerical scheme. By adding these two equations we obtain

$$r(t + \Delta t) + r(t - \Delta t) = 2r(t) + a(t)\Delta t^2 + O(\Delta t^4) \tag{2.16}$$

or

$$r(t + \Delta t) = 2r(t) - r(t - \Delta t) + a(t)\Delta t^2 + O(\Delta t^4) \tag{2.17}$$

This equation is known as the Verlet algorithm. The algorithm is properly centered, $r_i(t+\Delta t)$ and $r_i(t-\Delta t)$ play symmetrical roles, making it time-reversible and it shows excellent energy-conserving properties over long times. The algorithm assumes that the forces rely solely on the positional coordinates and not on the velocities. Although the velocities are not explicitly involved in the algorithm, they are necessary for calculating the kinetic energy and, consequently, the temperature. Velocity can be obtained by subtracting Eq. (2.14) with Eq. (2.15),

$$r(t+\Delta t) - r(t-\Delta t) = 2v(t)\Delta t + O(\Delta t^3) \tag{2.18}$$

or

$$v(t) = \frac{r(t+\Delta t) - r(t-\Delta t)}{2\Delta t} + O(\Delta t^2) \tag{2.19}$$

One limitation of the original Verlet algorithm is that it does not have a "self-starting" property. Usually the initial conditions are given at the same time, $r_i(0)$ and previous $r_i(-\Delta t)$ time steps. There is also some concerns (Dahlquist & Bjork, 1974) that roundoff errors may arise when implementing Eq. (2.17). The original Verlet algorithm, Eqs (2.17) and (2.19), do not handle the velocities in a fully satisfactory manner A Verlet-equivalent algorithm that stores positions, velocities, and accelerations at the same time and which also minimizes round-off errors was introduced. Consider Eq. (2.15) at the next time step,

$$r(t) = r(t+\Delta t) - v(t+\Delta t)\Delta t + \frac{1}{2}a(t+\Delta t)\Delta t^2 + ... \tag{2.20}$$

By adding these with Eq.(2.14) and solving for $v(t+\Delta t)$ yields,

$$v(t+\Delta t) = v(t) + \frac{1}{2}[a(t) + a(t+\Delta t)]\Delta t \tag{2.21}$$

Equation (2.21) represents the velocity Verlet algorithm, which is an equivalent formulation to the original Verlet algorithm. Both algorithms produce the same trajectories for the simulated system. The key advantage of the velocity Verlet algorithm is that it only requires the storage of positions, velocities, and accelerations at a single time point. This makes it computationally efficient and memory-efficient compared to other integration schemes.

2.9.2 Limitations of molecular dynamics

Like any simulation methods, molecular dynamics has its own set of drawbacks (Kwan et al., 2023). The system size restriction is one of the most obvious limits. This is especially important when simulating real-world materials with a broad range of length scales, from microns to one nanometer. Molecular dynamics can be used in combined with a more mesoscopic technique, like the Boltzmann Transport Equations, to handle such situations. This method uses the microscopic data about the phonon lifespan as an input to a Boltzmann transport equation. The classical nature of molecular dynamics is another drawback. Each phonon mode in this framework has an equal population, and the Dulong-Petit law provides a reasonable approximation of the heat capacity. For solids that are at or slightly above their Debye temperature, this approximation is accurate. But at room temperature, many materials don't follow this requirement (Durrant & McCammon, 2011). Many methods can be used to introduce quantum effects into molecular dynamics. One method is to use phonon lifetimes calculated from molecular dynamics in a Boltzmann transport equation where the phonon occupation number takes quantum statistics into account. Alternatively, a Langevin thermo-stat with colored noise that obeys a Bose-Einstein distribution for the phonon mode

can be used to directly incorporate quantum effects into the molecular dynamics simulation. Consequently, molecular dynamics does not explicitly simulate electronic degrees of freedom. As such, fundamental molecular dynamics cannot be used to study thermal transport in electrical conductors. Moreover, the basic form of molecular dynamics does not take into consideration the contribution of electron-phonon scattering to transport in semiconductors.

2.10. Predicting thermal conductivity Using Non Equilibrium molecular dynamics

A solid can transfer heat energy by a number of methods, including phonon conduction, electron conduction, and other excitations like spin waves (Tritt, 2005). There are three primary methods available for calculating thermal conductivity using molecular dynamics simulations. The equilibrium strategy, which uses the Green-Kubo formulas, is the first method. This method uses correlation functions to calculate the thermal conductivity while allowing the system to reach thermal equilibrium. The second method is the direct method or non-equilibrium molecular dynamics method. This method entails building a heat sink and a heat source inside the system. Temperature gradients and heat flow monitoring allow for the determination of thermal conductivity. The homogeneous non-equilibrium molecular dynamics method is the third technique. This method involves inducing a heat flux within the system and obtaining the thermal conductivity by analyzing the subsequent temperature distribution These methods based on molecular dynamics offer useful instruments for assessing a material's thermal conductivity, especially in semiconductor (Dong et al., 2018).

The trajectories and velocities of particles (such as atoms or molecules) in an MD simulation are found by the numerical solution of Newton's second law of motion. In this technique, a differential equation with initial and boundary conditions is solved for a particular number of particles, which can be anywhere from a few to millions. A potential energy function that is selected to replicate experimentally proven variables, such elastic constants and melting temperatures, describes the interaction between atoms or molecules. The potential for elements with covalent bonds is made up of two and three-body contributions. According to the Pauli exclusion principle, the two-body potential consists of a Lennard-Jones-like term with a repulsive short-range component originating from the overlap of atomic orbitals and a long-range attractive component owing to dipole-dipole interactions. The interatomic distance is determined by the two-body interaction, while the bonds between atoms organized in tetrahedral coordination are stabilized by the three-body potential. A certain process is taken to use NEMD simulation to ascertain a material's thermal conductivity (Termentzidis & Merabia, 2012). A temperature gradient is created along the sample since this method involves a non-equilibrium condition. The sample is placed between the hot and cold reservoirs to form the simulation cell. By rescaling the particle velocities inside the reservoirs, the temperature is regulated and the center of mass is kept from moving in a net translational direction. A temperature gradient forms along the sample as heat is introduced at the hot end and withdrawn at the cold end. A steady-state temperature gradient eventually develops; the length of the sample and the heat conductance determine this. The material's thermal conductivity is directly correlated with this steady-state gradient. The sample is cut into slices in order to compute the temperature profile required to identify the temperature gradient. The average kinetic energy of the atoms in each slice is used to calculate the temperature within it, under the assumption that local equilibrium makes the equipartition theorem applicable. The thermal conductivity of the sample is then calculated from the added amount of heat $\frac{dE}{dt}$

divided by the negative temperature gradient $\frac{dT}{dx}$ and the cross-section area A of the sample.

2.11. Classical Interatomic Potentials

The selection of appropriate classical interatomic potentials is vital for molecular dynamics (MD) predictions. It is also important for the potentials to have simplicity in order to enhance their transferability. Currently, there are no available simple interatomic potentials that adequately describe the interactions in Bi_2Te_3. While there are simple harmonic potentials fitted using experimental data (Kullmann et al., 1990), they are not suitable for calculating lattice thermal conductivity because they neglect anharmonic effects. On the other hand, Huang and Kaviany (Chen & Chen, 2005), have developed classical interatomic potentials that incorporate both two-body and three-body interactions, which can accurately replicate the phonon behavior of Bi_2Te_3. However, these potentials come with increased complexity (Qiu & Ruan, 2009). The two body potential $\phi(r_{ij})$ between atoms i and j separated by a distance r_{ij} can be written in a form consisting of a short-range interaction $\phi_s(r_{ij})$ and a Coulombic term for the long-range electrostatic interaction:

$$\phi(r_{ij}) = \frac{q_i q_j}{r_{ij}} + \phi_s(r_{ij}) \tag{2.22}$$

Where the first part is coulombic interaction and The second part is the short-range Morse potential given by,

$$\phi_s(r_{ij}) = D_e(1 - e^{[} - a(r_{ij} - r_0)]^2 - 1) \tag{2.23}$$

Here, D_e is the depth of the potential well, r_0 is the equilibrium bond distance, and a is the measure of bond elasticity.

2.12. Boltzmann Transport Equation

The Boltzmann Transport Equation is a theoretical framework used to analyze the transport of carriers in a semi-classical manner. It combines principles of classical Newtonian mechanics and quantum probabilistic scattering rates, known as the Fermi-Golden rule. This equation describes the trajectory of a particle by considering both its classical motion and the dissipative processes that occur as it transitions between different energy states (Banoo et al., 2000). The Boltzmann transport equation is analogous to Schrödinger's equation, but it describes the evolution of the electronic distribution function f, over time. This distribution function represents the probability of occupation of different electronic states. The Boltzmann transport equation is a robust and widely applicable equation that can be used to derive all of the essential transport parameters, making it a fundamental tool in the study of electronic transport phenomena (Nolting, 2012). To characterize the transport properties of an electron, it is necessary to understand the distribution function of the electrons. This distribution function provides information about how the electrons are distributed in momentum space (also known as k-space) and energy space. By analyzing this distribution, we can evaluate various transport properties. In equilibrium conditions, the distribution function can be described by the Fermi-Dirac function,

$$f(\varepsilon) = \frac{1}{exp(\frac{\varepsilon(k)-\mu}{K_B T}) + 1} \tag{2.24}$$

where T is the absolute temperature, $\varepsilon(k)$ is the electron energy, k_B is the Boltzmann constant, and μ the chemical potential (the Fermi energy at 0 K) (Cantarero & Àlvarez, 2014). The equilibrium electron gas is characterized by this distribution function. Even if collisions constantly remove electrons from one k-state to another, the Fermi-Dirac function will always supply the net distribution of electrons as long as there are no external variables that could upset the equilibrium. To describe the distribution function in the presence of external forces, let's denote $f_k(r)$ as the local concentration of electrons in state k in the neighborhood of position r. The Boltzmann approach involves investigating how $f_k(r)$ changes over time.

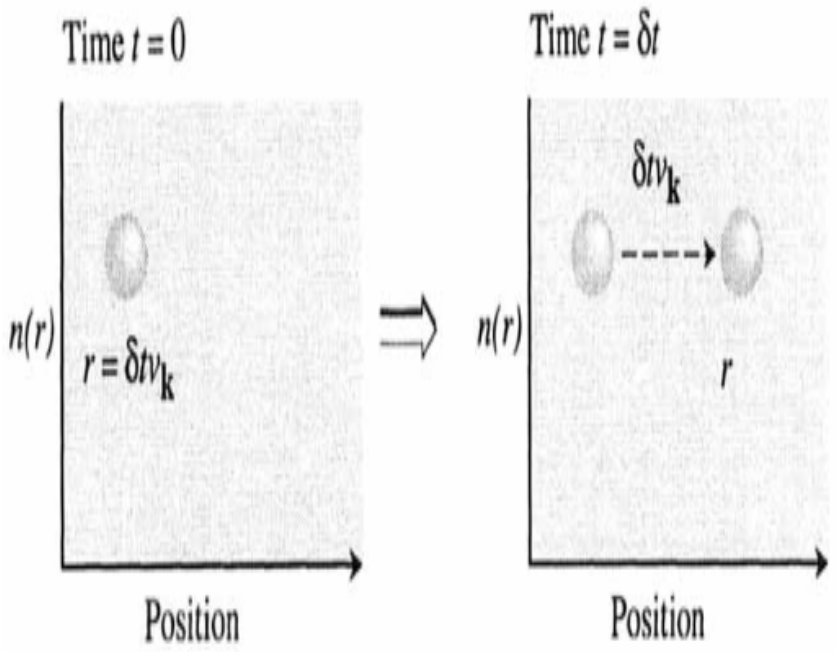

Figure 2.6: At time t = 0 particles at position $r - \delta t V_k$ reach the position r at a later time δt (J. Singh, 2008).

The variation in the electron distribution function $f_k(r)$ can be explained by three main factors (J. Singh, 2008). Firstly, as a result of the continuous diffusion of electrons, carriers will constantly enter and exit any given volume element around a specific position r. Secondly, when external forces are applied to electrons in a material, the electrons will alter their momentum (or wavevector) according to $\hbar dk/dt = F_{ext}$. Thirdly, as a result of various scattering processes, electrons in a material undergo transitions from one k-state (momentum state) to another.

To compute the total time derivative of the distribution function $f_k(r)$, we can break it down into the three main contributing factors discussed above.

2.12.1 The evolution of $f_k(r)$ induced by diffusion

The electron will traverse $v_k t$ distance in a time interval t if v_k is the velocity of a carrier in state k. Therefore, as shown in Figure 2.6, the number of carriers in the neighborhood of $r - \delta t V_k$ at time 0 will be equal to the number of electrons in the vicinity of r after time δt. Diffusion allows us to prove the following equality (J. Singh, 2008),

$$f_k(r, \delta t) = f_k(r - \delta t v_k, 0) \tag{2.25}$$

Using a Taylor series, let's expand the electron distribution functions $f_k(r, \delta t)$ and $f_k(r - \delta t v_k, 0)$;

$$f_k(r, \delta t) \approx f_k(r) + \frac{\partial f_k(r)}{\partial t}\delta t + \frac{1}{2}\frac{\partial^2 f_k(r)}{\partial t^2}(\delta t)^2 + ... \tag{2.26}$$

and

$$f_k(r - \delta t v_k, 0) \approx f_k(r,0) - \frac{\partial f_k}{\partial t}(r,0)(\delta t v_k) + \frac{1}{2!}\frac{\partial^2 f_k}{\partial t^2}(r,0)(\delta t v_k)^2 - \dots \tag{2.27}$$

by ignoring terms of a higher order, We can write Eqn (2.25) as follows

$$f_k(r,0) + \frac{\partial f_k}{\partial t}.\delta t = f_k(r,0) - \frac{\partial f_k}{\partial t}.\delta t v_k \tag{2.28}$$

Moreover, the above equation is simplified to

$$\frac{\partial f_k}{\partial t}_{(diff)} = -\frac{\partial f_k}{\partial t}.v_k \tag{2.29}$$

2.12.2 The evolution of $f_k(r)$ induced by an external field

By Newton's equation of motion, the crystal momentum k of an electron varies in response to external forces. For an electric and magnetic field (E and B), the rate of change of k is given by

$$\dot{\mathbf{k}} = \frac{e}{\hbar}[(\mathbf{E} + \mathbf{v_k} \times \mathbf{B})] \tag{2.30}$$

By drawing a comparison with the changes brought about by diffusion, we may suggest that at time $t = 0$, particles having momentum $k - \dot{k}$ will have momentum $\mathbf{k}$ at time δt, and

$$f_k(r, \delta t) = f_{k - \dot{k}\delta t(r,0)} \tag{2.31}$$

By Tylor series expansion now

$$f_k(r, \delta t) \approx f_k(r) + \frac{\partial f_k(r)}{\partial t}\delta t + \frac{1}{2}\frac{\partial^2 f_k(r)}{\partial t^2}(\delta t)^2 + ... \tag{2.32}$$

$$f_{k - \dot{k}\delta t}(r,0) \approx f_k(r,0) - \dot{k}\delta t\frac{\partial f_k}{\partial k}(r,0) + \frac{1}{2}(\dot{k}\delta t)^2\frac{\partial^2 f_k}{\partial k^2}(r,0) - \dots \tag{2.33}$$

In this case, as well, eliminating the higher order terms from the expansion and substituting into Eqn (2.31) yields

$$\begin{aligned}\frac{\partial f_k}{\partial t}_{(ext.forces)} &= -\dot{k}\frac{\partial f_k}{\partial k} \\ &= \frac{-e}{\hbar}[(\mathbf{E}+\frac{\mathbf{v}\times\mathbf{B})}{c}].\frac{\partial f_k}{\partial k}\end{aligned} \tag{2.34}$$

2.12.3 The evolution of the function $f_k(r)$ due to scattering

Let us assume that, the scattering processes are considered to be local and instantaneous, resulting in a change in the electron's state from k to k'. The rate of change of the distribution function $f_k(r)$ due to scattering can be defined by the function $W(k,k')$ which represents the rate of scattering from state k to k' when state k is occupied and state k' is empty (J. Singh, 2008).

$$\frac{\partial f_k}{\partial t}_{scattering} = \int [f'_k(1-f_k)W(k',k) - f_k(1-f'_k)W(k,k')]\frac{d^3k'}{(2\pi)^3} \tag{2.35}$$

The term $(2\pi)^3$ in the denominator arises from the number of allowed states in a k-space volumee element, represented by d^3k'. The first term in the integral corresponds to the rate at which electrons transition from an occupied k' state (indicated by the factor f'_k) to an unoccupied k state (indicated by the factor $(1-f_k)$). On the other hand, the second term represents the term related to the loss of electrons.

In a steady-state condition, the distribution function remains constant, and as a result, the sum of the partial derivative terms calculated earlier will be zero, indicating no net change in the distribution function.

$$\frac{\partial f_k}{\partial t}_{scattering} + \frac{\partial f_k}{\partial t}_{diff} + \frac{\partial f_k}{\partial t}_{ext.forces} = 0 \tag{2.36}$$

let us introduce

$$g_k = f_k - f_k^0 \tag{2.37}$$

where f_k^0 is the equilibrium distribution. Now let us compute g_k, which quantifies the deviation of the distribution function from the equilibrium state.

By substituting the partial time derivatives resulting from diffusion and external fields, the resulting expression is given by:

$$-v_k.\nabla_r f_k - \frac{e}{\hbar}[(\mathbf{E}+\frac{\mathbf{v_k}\times\mathbf{B})}{c}].\nabla_k f_k = -\frac{\partial f_k}{\partial t}_{scattering} \tag{2.38}$$

By Replacing $f_k = g_k + f_k^0$

$$\begin{aligned}&-v_k.\nabla_r f_k^0 - \tfrac{-e}{\hbar}[(\mathbf{E}+\mathbf{v_k}\times\mathbf{B})].\nabla_k f_k^0 \\ &= -\frac{\partial f_k}{\partial t}_{scattering} + v_k.\nabla_r g_k + \frac{e}{\hbar}[(\mathbf{E}+\mathbf{v_k}\times\mathbf{B})].\nabla_k g_k\end{aligned} \tag{2.39}$$

It is worth noting that the magnetic force term on the left-hand side of Eqn.2.39 is directly

proportional to

$$v_k . \frac{e}{\hbar}(\mathbf{v_k} \times \mathbf{B})$$

and is thus zero. Let us recall

$$v_k = \frac{1}{\hbar}\frac{\partial \varepsilon(k)}{\partial k} \tag{2.40}$$

Here $\varepsilon(k)$ is the energy of the particle and μ is chemical potential. Then the equilibrium distribution f_k^0 given by;

$$f_k^0 = -\frac{1}{exp[\frac{\varepsilon(k)-\mu}{k_B T}]+1} \tag{2.41}$$

consequently

$$\nabla_r f^0 = -\frac{[exp\frac{(\varepsilon(k)-\mu)}{k_B T}]}{[exp(\frac{\varepsilon(k)-\mu}{k_B T})+1]^2}\nabla_r(\frac{\varepsilon(k)-\mu(r)}{k_B T(r)})$$

$$= k_B T.\frac{\partial f^0}{\partial \varepsilon(k)}[-\frac{\nabla\mu}{k_B T} - \frac{(\varepsilon(k)-\mu)}{k_B T^2}\nabla T]$$

$$\nabla_r f^0 = \frac{\partial f^0}{\partial \varepsilon(k)}[-\nabla\mu - \frac{\varepsilon(k)-\mu}{T}\nabla T] \tag{2.42}$$

Furthermore

$$\nabla_k f^0 = \frac{\partial f^0}{\partial \varepsilon(k)}\nabla_k \varepsilon(k)$$

$$= \hbar v_k \frac{\partial f^0}{\partial \varepsilon(k)} \tag{2.43}$$

We obtain, from Eqn. 2.39, by substituting these terms and keeping only terms that are second-order in the electric field (i.e., disregarding terms involving products $g_k.E$).

$$-\frac{\partial f^0}{\partial \varepsilon(k)}.v_k.[-\frac{(\varepsilon(k)-\mu)}{T}\nabla T + eE - \nabla\mu] \tag{2.44}$$

$$= -\frac{\partial f}{\partial t}_{scattering} + v_k.\nabla_r g_k + \frac{e}{\hbar}(\mathbf{v_k} \times \mathbf{B}).\nabla_k g_k \tag{2.45}$$

The derived above equation is called Boltzmann transport equation. We can utilize this equation to derive expressions for transport properties of the material.

3. METHODOLOGY

3.1. Model and Non-equilibrium molecular dynamics (NEMD) Simulation Method

3.1.1 Thermoelectric generator Model

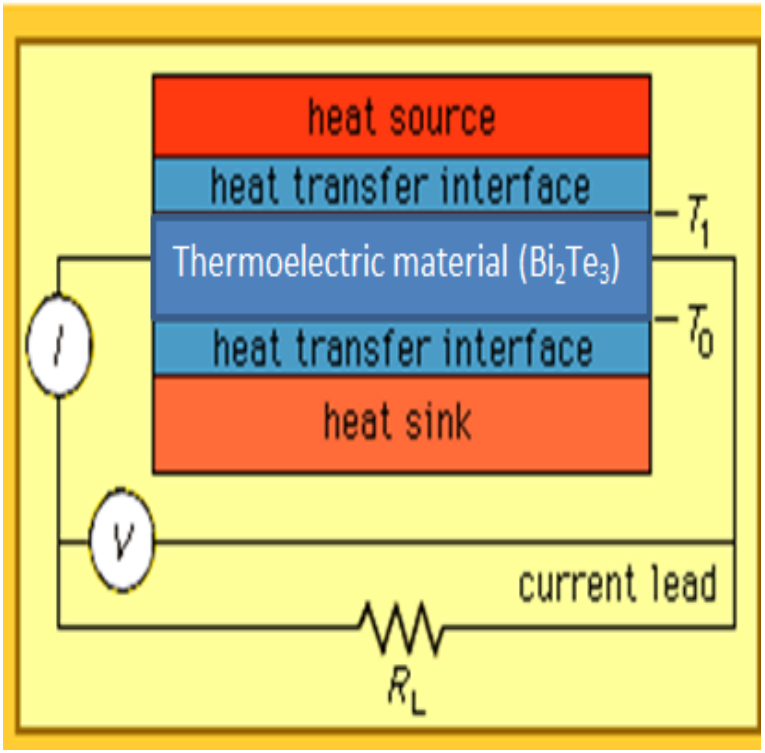

Figure 3.1: Model of Thermoelectric generator (Mary-Rose & Wallenfeldt, 2024).

A thermoelectric generator consists of several components that work together to convert heat energy into electrical energy. These components play distinct roles in the overall energy generation process. The heat source serves as the initial supplier of thermal energy to the TEG. It can be a combustion engine, waste heat from an industrial process or a solar collector. The heat source provides the necessary heat input to the device, typically on the high-temperature side. The heat transfer interface is responsible for facilitating the efficient transfer of heat from the heat source to the thermoelectric material. This interface is designed to maximize heat conduction and minimize thermal losses. The thermoelectric material is the core component of the device. It is a semiconductor material (Bi_2Te_3) with unique properties that enable it to convert heat into electricity through the thermoelectric effect. The material possesses a Seebeck coefficient, which determines its ability to generate an electric voltage when subjected to a temperature gradient. When a temperature difference is applied across the material, it induces the migration of charge carriers (electrons or holes) from the hot side to the cold side, resulting in the generation of an electric potential difference. This potential difference drives an electric current when an external load, such as a load resistor, is connected.

The heat sink is in thermal contact with the cold side of the thermoelectric material. Its purpose is to dissipate or absorb the waste heat generated during the energy conversion process. By removing excess heat, the heat sink helps maintain a temperature difference across the device, ensuring its efficient operation and preventing thermal equilibrium. The load resistor is an external electrical load connected to the thermoelectric device. It consumes the electrical power generated by the thermoelectric material. When an electric current flows through the load resistor, a voltage drop occurs, resulting in the conversion of heat energy into useful electrical energy. The load resistor can be part of a larger electrical circuit or a device that utilizes the generated electricity for various applications. In general, TEG utilizes the heat source to supply thermal energy, transfers heat via the heat transfer interface, converts heat to electricity through the thermoelectric material, dissipates waste heat with the heat sink, and finally, consumes electrical power with the load resistor. Together, these components enable the conversion of heat energy into electrical energy in a TEG.

3.1.2 Computational Method

In molecular dynamics (MD) simulation, the behavior of atoms is dictated by Newton's second law, which relates the forces acting on each atom to its motion. These forces, in turn, are determined by the positions of the atoms and the molecular force fields associated with them. The equations of motion are integrated by the Velocity-verlet algorithm, which computes displacement, velocity and acceleration of each atom every time step.

In this work thermal conductivity of Bi_2Te_3 was calculated using NEMD method implemented in the LAMMPS software. The simulation comprised of three distinct stages as depicted in Figure 3.3. The first stage of the simulation involved the relaxation of the Bi_2Te_3 system. The initial Bi_2Te_3 structure was loaded into LAMMPS, and periodic boundary conditions were applied to the simulation box. A NVT (constant volume and temperature) ensemble simulation was then run for 100 time steps to allow the system to reach thermal equilibrium. During this stage, the temperature, energy, and other relevant properties were monitored to ensure the system had reached a steady state. The second stage of the simulation involved the isothermal control of the system. The simulation box was divided into two regions: a "hot" region and a "cold" region as shown in Figure 3.2. A heat energy was then added to the system in the z-direction to the atoms in the hot region. A NVE (constant volume and energy) ensemble simulation was then run for 10,000 time steps to allow the system to reach a steady-state temperature gradient. The final stage of the simulation involved the heat conduction analysis. During this stage, the temperature profile along the z-direction of the simulation box was monitored to ensure a linear temperature gradient had been established. The heat flux was calculated based on the energy added to the hot region and removed from the cold region. Using Fourier's law, the thermal conductivity of the bismuth telluride system was then calculated from the temperature gradient and the heat flux.

$$\kappa_l = -\frac{J_z}{\frac{\partial T}{\partial z}} \tag{3.1}$$

where, J_z is heat flux, κ_l is lattice thermal conductivity of the material and $\frac{\partial T}{\partial z}$ is the temperature gradient across the material. The negative sign indicates that heat flows from the hot to the cold region.

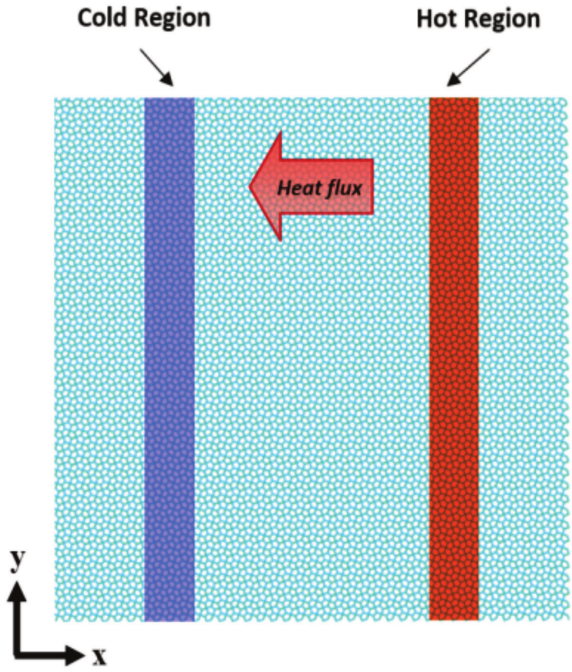

Figure 3.2: The Two Region Method Model utilized in the NEMD simulation (Muna & Winczewski, 2020)

.

3.2. Boltzmann Transport Equation (BTE)

The Boltzmann Transport Equation is a fundamental equation in statistical mechanics that describes the behavior of particles (such as electrons or phonons) in a material under the influence of an external field, such as an electric field or a temperature gradient. BTE provides a theoretical framework to understand and predict how charge carriers and heat are transported within the material. It describes the probability distribution of particles in momentum space and provides a mathematical description of their scattering processes, interactions, and transport behavior.

In this work, the electron transport properties such as electronic thermal conductivity, electrical conductivity, and Seebeck coefficient of the material were calculated by the semi-classical Boltzmann transport theory within the constant relaxation time approximation (CRTA) approach as implemented in the BoltzTraP code. The electron transport calculations flowchart and employed programs are schematically displayed in Figure 3.4. The BoltzTraP code utilizes interpolation techniques and conducts necessary integrations to solve the Boltzmann equation (Eqn 2.45) and gives the electronic property of the material. Over the past ten years, the BoltzTraP code has been tested on a variety of materials, including thermoelectric materials and superconductors (Allen et al., 1988). In several situations, there was good agreement with the experimental values (Madsen et al., 2003). Notably, the BoltzTraP code's shortcoming caused the phonon contribution to thermal conductivity to be disregarded, resulting in a minor overestimation of the ZT values observed here. Only the electronic portion of the thermal conductivity is provided by the BoltzTraP code, which treats the lattice thermal conductivity contributed by phonons as a constant.

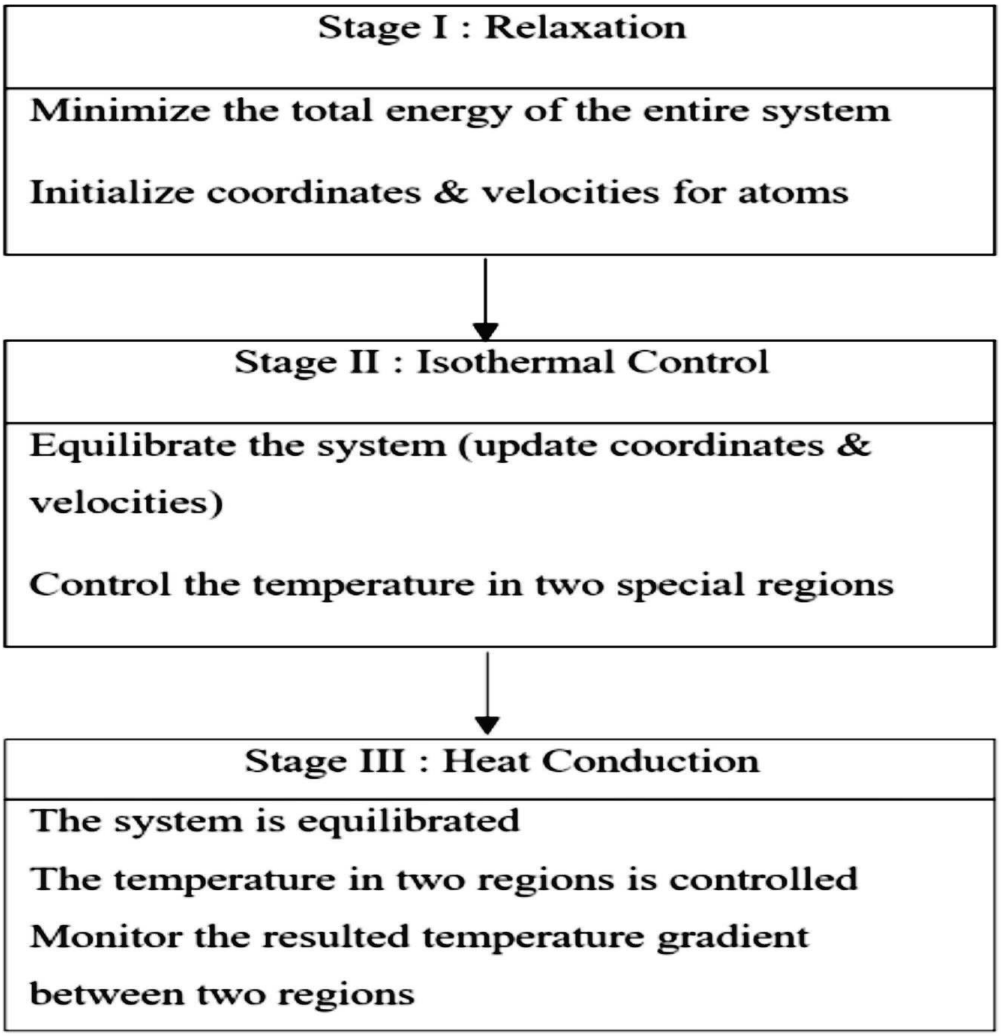

Figure 3.3: NEMD simulation structure flowchart illustrating how to compute thermal conductivity (Muna & Winczewski, 2020).

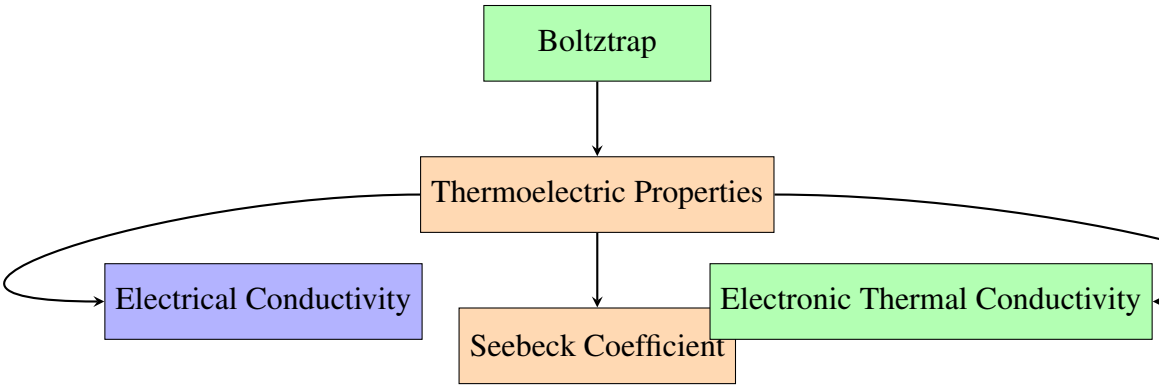

Figure 3.4: Schematic of the flow chart for electronic transport properties.

3.3. Efficiency of thermoelectric generator

The technique for calculating the efficiency of a thermoelectric generator using the material Bi_2Te_3 involves a series of interconnected steps as shown in Figure 3.5 below. The process begins by selecting Bi_2Te_3 as the material of interest. To gather the information required for the computations, two parallel routes are taken.

The first route involves employing the Non-Equilibrium Molecular Dynamics (NEMD) method. NEMD simulations are conducted using the LAMMPS software, which provides data on the lattice thermal conductivity of Bi_2Te_3. This data is crucial for subsequent calculations. The second route involves utilizing the Boltzmann Transport Equation (BTE) method. The BTE calculations are performed using the BoltzTrap software, which provides data on the electronic thermal conductivity, electrical conductivity, and Seebeck coefficient of Bi_2Te_3. These parameters play a significant role in determining the thermoelectric properties of the material. The results obtained from both the NEMD and BTE methods are combined to calculate the Figure of Merit of Bi_2Te_3 through Eqn 2.9. Finally, the figure of merit is utilized to calculate the overall efficiency of the thermoelectric generator by monitoring sink and source temperature of the device.

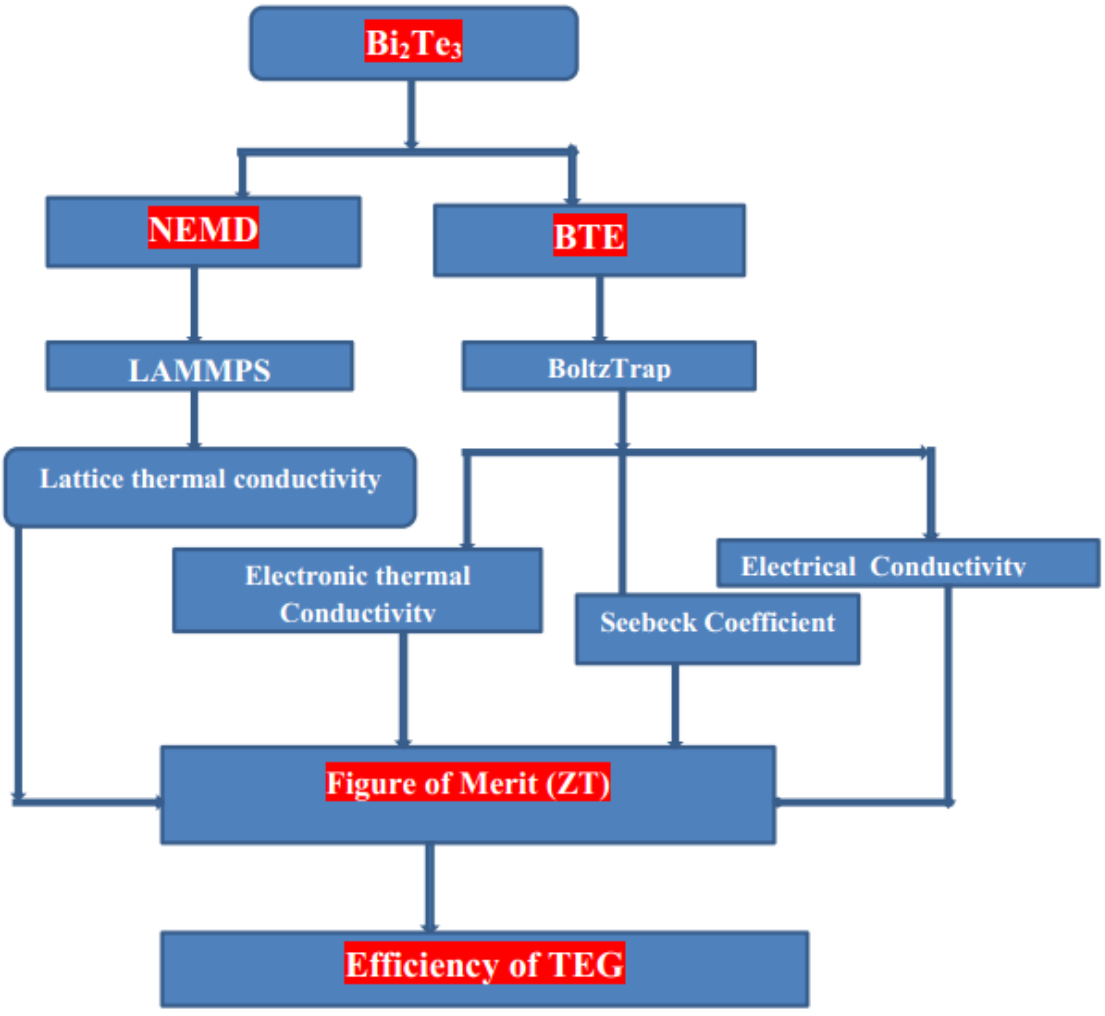

Figure 3.5: Thermoelectric Generator Efficiency Calculation Flowchart.

3.4. softwares

We utilized the LAMMPS software, an acronym for "Large-scale Atomic/Molecular Massively Parallel Simulator," to conduct non-equilibrium molecular dynamics simulations. Developed by the Sandia National Laboratories, LAMMPS is an open-source code specifically designed for molecular dynamics simulations, with a particular emphasis on material modeling. Its capabilities are particularly well-suited for solid-state materials such as metals and semiconductors, enabling atomistic or parallel particle simulations at both the atomic and continuum scales. LAMMPS offers significant potential in the realm of solid-state materials research (Wu et al., 2016). BoltzTraP software package is used to calculate the electronic transport properties of the material. Additionally, gnuplot was used for plotting purposes.

4. RESULTS AND DISCUSSION

4.1. Non-equilibrum molecular dynamics (NEMD) Simulation Result

4.1.1 Lattice thermal conductivity (κ_l)

For the system's temperatures of 100K, 200K, 300K, 400K, 500K, 600K, 700K, and 800K, the bulk Bi_2Te_3 lattice (Phonon) thermal conductivity has been computed by Non-equilibrium molecular dynamics method using LAMMPS software package and presented in Table 4.1. In this work, the room temperature lattice thermal conductivity of bismuth telluride (Bi_2Te_3) was predicted using the non-equilibrium molecular dynamics (NEMD) method and found to be approximately 1.37 W/m-K. This predicted value has been compared with the available experimental and theoretical data reported in the literature. The experimental measurement of the lattice thermal conductivity of Bi_2Te_3 at room temperature by Goldsmid (H. Goldsmid, 1956) yielded a value of around 1.5 W/m-K. The NEMD-predicted value of 1.37 W/m-K in the current study is in good agreement with the experimental data, with a deviation of only 8.7%. This small variation can be attributed to measurement techniques employed in the respective studies. Furthermore, the theoretical study by Qiu and Ruan (Qiu & Ruan, 2009) on the lattice thermal conductivity of Bi_2Te_3 using first-principles calculations reported a room temperature value of around 1.3 W/m-K. The NEMD-predicted value of 1.37 W/m-K in the present work is in close agreement with this theoretical prediction, with a deviation of only 5.4%. The close match between the predicted and theoretical values suggests that the current NEMD-based study has successfully captured the material properties governing the lattice thermal transport in Bi_2Te_3. The consistency between the NEMD-predicted room temperature lattice thermal conductivity and both the experimental data by Goldsmid and the theoretical prediction by Qiu and Ruan strengthens the confidence in the reliability and accuracy of the results presented in this work. This agreement also highlights the potential of the NEMD computational approach employed in the current study to provide valuable insights into the thermal transport properties of Bi_2Te_3. The accurate prediction of lattice thermal conductivity is crucial for the design and optimization of thermoelectric devices, as it directly influences the figure of merit (ZT) and the overall efficiency of the thermoelectric generator. The close alignment of the NEMD-predicted value with the experimental and theoretical literature data emphasizes the validity of the present work.

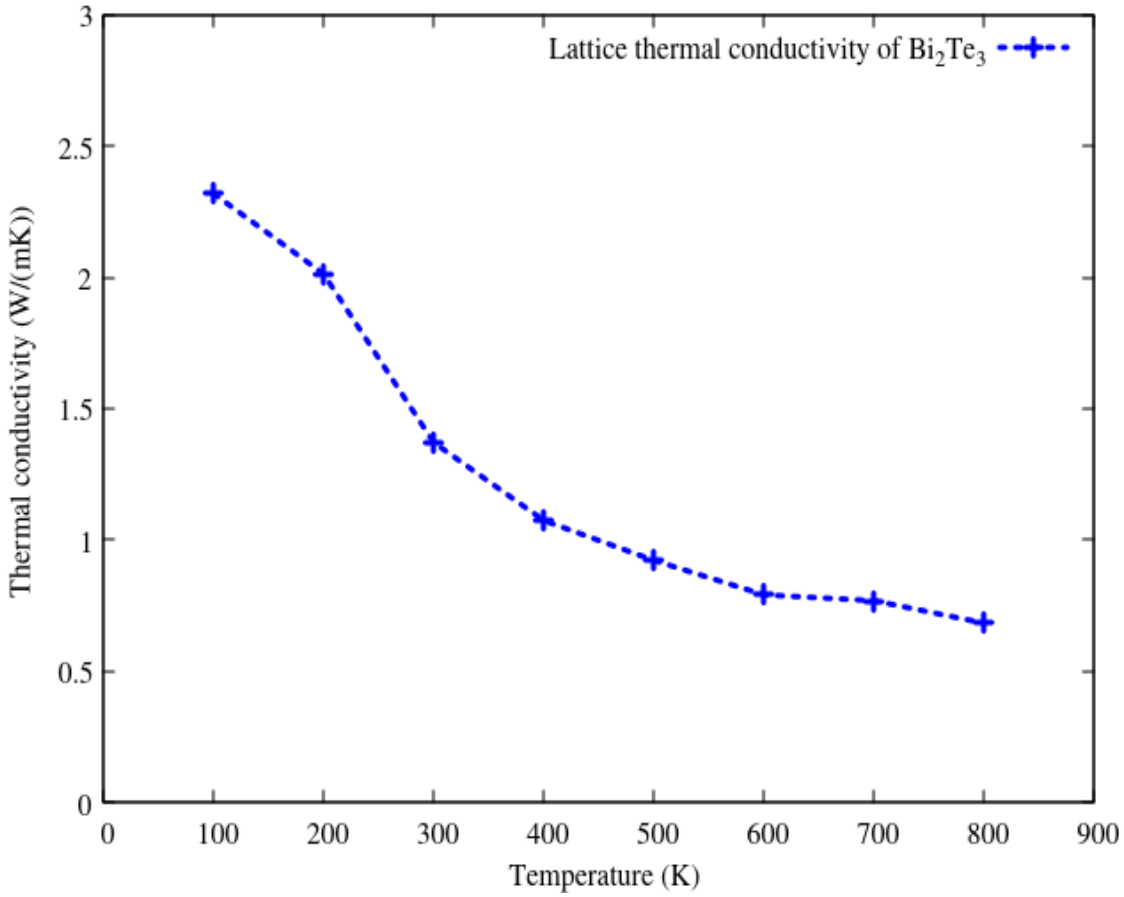

Figure 4.1: Temperature Dependence of lattice thermal conductivity of Bi_2Te_3

Figure 4.1 shows the temperature dependence of lattice thermal conductivity of bulk Bi_2Te_3. The graph demonstrates that as the temperature of a material increases, the lattice thermal conductivity tends to decrease. This phenomenon can be attributed to the stronger phonon scattering that occurs at higher temperatures. Phonons, which are quantized lattice vibrations responsible for carrying heat energy in a material, become more vigorous and energetic as the temperature rises. The intensified lattice vibrations lead to a greater tendency for phonons to interact with various scattering mechanisms present within the material. These scattering mechanisms can include impurities, defects, boundaries, and other imperfections in the lattice structure. When phonons collide with these scattering centers, their smooth propagation is disrupted, resulting in a decrease in thermal conductivity. At elevated temperatures, the phonons experience a higher frequency of collisions with the scattering centers. This increased scattering hinders the efficient transfer of heat energy through the material. The disrupted phonon flow prevents the smooth propagation of heat, leading to a reduction in thermal conductivity. The underlying reason for this decrease lies in the obstructed pathway of the phonons.

The more vigorous lattice vibrations at higher temperatures provide more opportunities for phonons to collide and scatter, impeding their smooth propagation. As a result, the material's ability to conduct heat decreases, and its thermal conductivity is reduced. Remarkably, this reduction in thermal conductivity can have practical advantages in thermoelectric applications. In these applications, materials with low thermal conductivity are preferred because they allow for better heat retention and enable a higher temperature gradient across

the material. By decreasing the thermal conductivity, the material can better retain the heat, which enhances the efficiency of thermoelectric conversion processes. The higher temperature gradient across the material facilitates improved energy conversion, leading to enhanced performance in thermoelectric applications.

Table 4.1: The calculated lattice thermal conductivity of Bi_2Te_3

Temperature (K)	Thermal conductivity (W/mK)
100	2.31852
200	2.01267
300	1.37122
400	1.07467
500	0.98273
600	0.79181
700	0.76944
800	0.68330

4.2. Boltzmann transport equation (BTE) Results

All transport properties of Bi_2Te_3 thermoelectric material such as electronic thermal conductivity, electrical conductivity, and Seebeck coefficient were obtained from BTE with constant relaxation time approximation from the reference (Mili et al., 2022) by using Boltztrap software.

Table 4.2: Electron transport properties of Bi_2Te_3

Temperature (K)	$\kappa_e(W/mK)$	$\sigma(1/\Omega m)$	S (V/K)
100	0.36969	121552.5	0.000112
200	0.8177	115096.5	0.0001442
300	1.39	110175	0.00016
400	2.067	104952	0.000176
500	3.173835	103307.5	0.0001933
600	4.494	102505	0.00021
700	5.813	101162	0.0002252
800	6.8111	100537	0.000237

4.2.1 Electronic thermal conductivity (κ_e) of Bi_2Te_3

The graph in Figure 4.2 depicts the temperature dependence of the electronic thermal conductivity in the thermoelectric material Bi_2Te_3. The observed trend reveals that as the temperature increases, the electronic thermal conductivity of Bi_2Te_3 also increases. At lower temperatures, the electronic thermal conductivity of Bi_2Te_3 is relatively low. This can be attributed to the limited thermal excitation of charge carriers and the less prominent energy-dependent scattering processes that facilitate heat conduction through electrons. In this temperature regime, the lattice thermal conductivity, which is the transfer of heat through the vibrations of the crystal lattice, may play a more dominant role in the overall thermal transport behavior of the material. However, as the temperature rises, the electronic thermal conductivity of Bi_2Te_3 demonstrates a significant increase. This can be explained by two key

mechanisms. Firstly, at higher temperatures, more electrons in the material are thermally excited into higher energy states, leading to a greater concentration of charge carriers available for heat conduction through electronic processes. This enhanced charge carrier population facilitates the transfer of thermal energy, resulting in the observed increase in electronic thermal conductivity. Secondly, elevated temperatures also promote the occurrence of energy-dependent scattering mechanisms, such as electron-electron and electron-phonon scattering. These scattering events play a crucial role in the transfer of energy between the charge carriers, thereby enhancing the material's ability to conduct heat. The temperature-dependent increase in the electronic thermal conductivity has important implications for the overall thermal conductivity of Bi_2Te_3. Since the electronic contribution represents a significant portion of the total thermal conductivity at higher temperatures, thus the rise in the electronic component leads to an increase in the material's overall thermal conductivity.

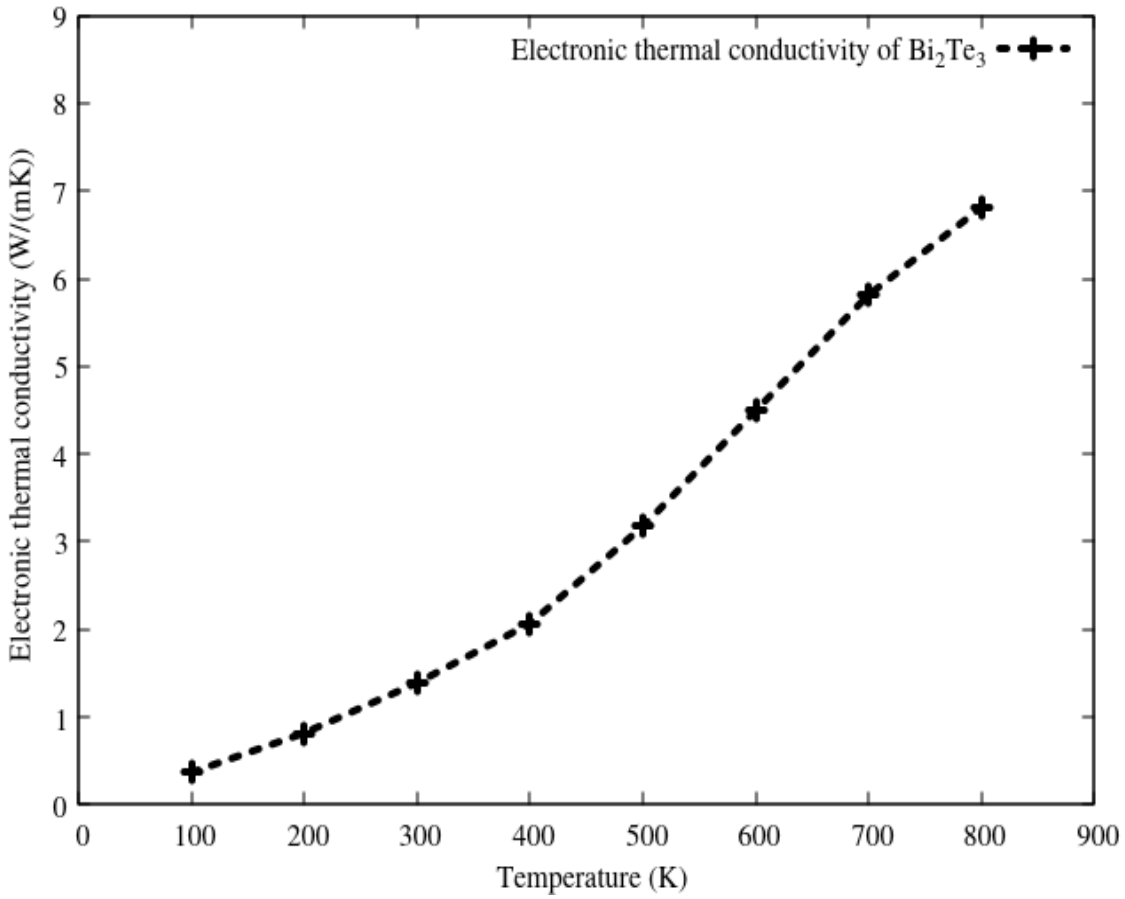

Figure 4.2: Temperature Dependence of electronic thermal conductivity of Bi_2Te_3

4.2.2 Total thermal conductivity (κ_T) of Bi_2Te_3

The plot of total thermal conductivity of Bi_2Te_3 with respect to temperature is shown in Fig. 4.3. The total thermal conductivity of Bi_2Te_3 increases as temperature increases. This is because, at low temperatures, the electronic thermal conductivity of Bi_2Te_3 is relatively low due to the dominance of phonon-mediated thermal transport. Particularly in the temperature range of 100-400k, the increasing rate of total thermal conductivity is relatively slow, this is due to the dominance of phonon thermal conductivity at lower temperatures. As the temperature rises, electronic thermal conductivity becomes increasingly significant in materials. This phenomenon can be attributed to the thermally induced excitation of electrons to higher energy states, leading to an increased population of charge carriers that are available for the conduction of heat. At higher temperatures, more electrons acquire sufficient energy to participate in heat conduction processes.

Moreover, when temperatures rise, the impact of energy-dependent scattering mechanisms becomes increasingly noticeable. The efficiency of heat transport within the material is largely determined by these mechanisms, which include electron-electron and electron-phonon scattering. Elevated temperatures lead to more frequent and powerful interactions between electrons and other particles or lattice vibrations, which intensify the scattering events. The overall increase in electronic thermal conductivity with temperature is facilitated by these scattering events, which also help to transport thermal energy between charge carriers. Consequently, as the temperature rises, electronic contribution to its thermal conductivity rises as well, increasing the total material's thermal conductivity overall.

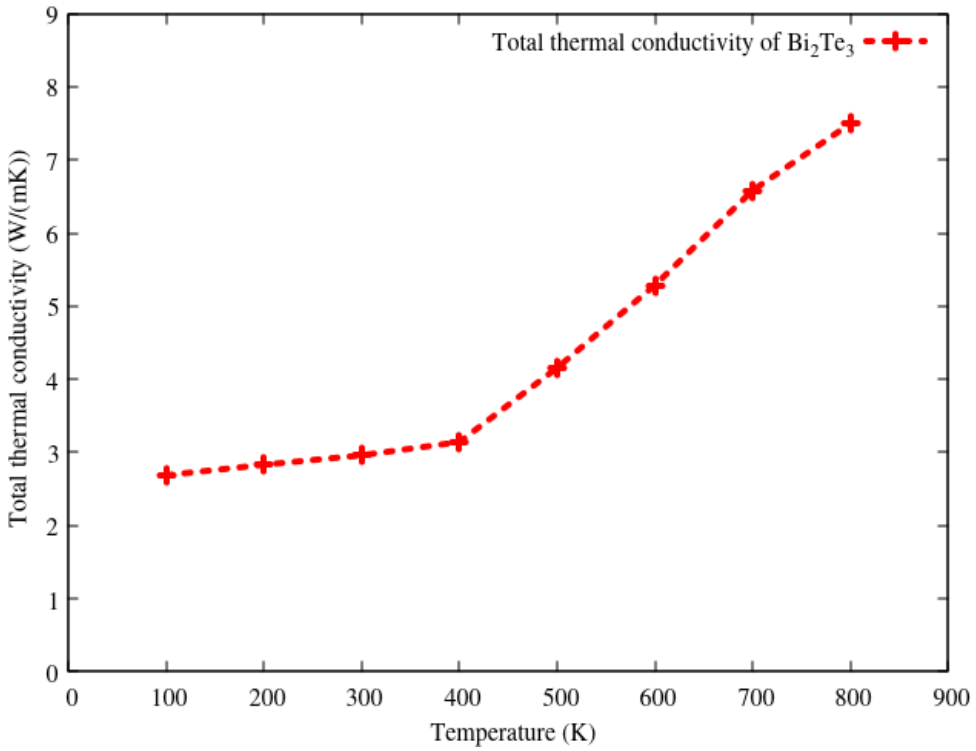

Figure 4.3: Total thermal conductivity of Bi_2Te_3

4.2.3 Electrical conductivity (σ) of Bi_2Te_3

The investigation into the thermal effect on the electrical conductivity of the thermoelectric material Bi_2Te_3 has yielded significant findings, which are illustrated in the corresponding graph (Figure 4.4). The graph demonstrates a distinct trend in the electrical conductivity of Bi_2Te_3 as a function of temperature. At low temperatures, the graph shows a relatively high electrical conductivity of Bi_2Te_3. This result suggests that at lower temperatures, the limited thermal energy restricts the number of charge carriers available to conduct electric current, resulting in a reduced population of carriers accessible for electrical conduction. However, the small number of available charge carriers possess high mobility, contributing to the relatively high electrical conductivity observed at low temperatures.

In contrast, as the temperature increases, the graph indicates a decrease in the electrical conductivity of Bi_2Te_3. This decrease can be attributed to the interplay between temperature and lattice vibrations. With increasing temperature, the thermal energy becomes sufficient to stimulate a larger number of charge carriers accessible to conduct electric current. However, as the temperature continues to rise, the enhanced thermal energy also intensifies lattice vibrations or phonons within the material. These phonons act as scattering centers for charge carriers, impeding their motion and reducing their mobility. Consequently, the dominant effect of phonon scattering exceeds the increase in charge carrier population, resulting in a decrease in electrical conductivity at higher temperatures. The observed temperature dependence of the electrical conductivity in Bi_2Te_3 has important implications for the material's performance in thermoelectric applications. The interplay between charge carrier concentration, carrier mobility, and phonon scattering at different temperature regimes determines the overall electrical conductivity of Bi_2Te_3, which is a crucial factor in the efficiency of thermoelectric energy conversion. At low temperatures, the relatively high electrical conductivity is advantageous for efficient charge transport and energy conversion. However, as the temperature increases, the decrease in electrical conductivity due to the dominant effect of phonon scattering can have a detrimental impact on the thermoelectric figure of merit. Understanding this temperature-dependent behavior is essential for optimizing the performance of Bi_2Te_3 in thermoelectric devices.

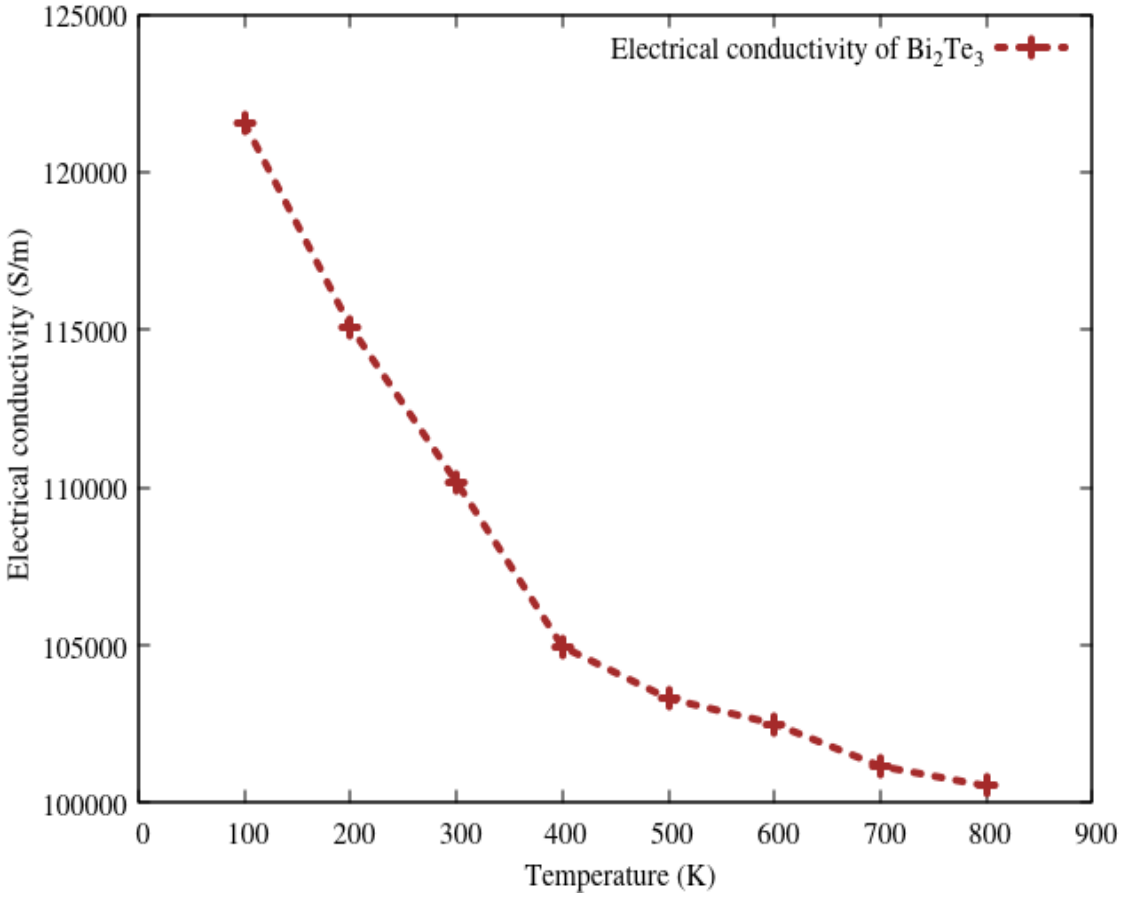

Figure 4.4: Electrical conductivity of Bi_2Te_3

4.2.4 Seebeck coefficient (S) of Bi_2Te_3

The Seebeck coefficient, also known as the thermopower, is a crucial parameter that quantifies the ability of a material to convert a temperature difference into an electrical voltage. The temperature dependence of the Seebeck coefficient in Bi_2Te_3 is shown in Figure 4.5. The majority of charge carriers in Bi_2Te_3 are electrons, and their behavior dominates the electrical transport properties. When a temperature gradient is applied across the material, the diffusion of these electrons from the hot side to the cold side creates a charge imbalance, resulting in the buildup of potential differences across the material. The magnitude of this voltage is proportional to the Seebeck coefficient. However, at low temperatures, the Seebeck coefficient of Bi_2Te_3 is typically small as the energy distribution of electrons in the material is relatively sharp, and only a small number of electrons possess sufficient energy to contribute to the thermoelectric effect. As the temperature increases, the energy distribution of electrons in Bi_2Te_3 broadens, allowing a larger number of charge carriers to participate in the thermoelectric process. This increase in the number of electrons contributing to the thermoelectric effect leads to a larger voltage generated per unit temperature gradient, resulting in a typically higher Seebeck coefficient at elevated temperatures as shown in Figure 4.5.

The temperature-dependent behavior of the Seebeck coefficient in Bi_2Te_3 is crucial in determining the material's overall thermoelectric performance. The increase in the Seebeck coefficient with rising temperature can have a positive impact on the thermoelectric figure of merit, a key parameter that governs the efficiency of thermoelectric energy conversion. This understanding of the temperature-dependent Seebeck coefficient in Bi_2Te_3 provides valuable insights for optimizing the material's performance in thermoelectric applications.

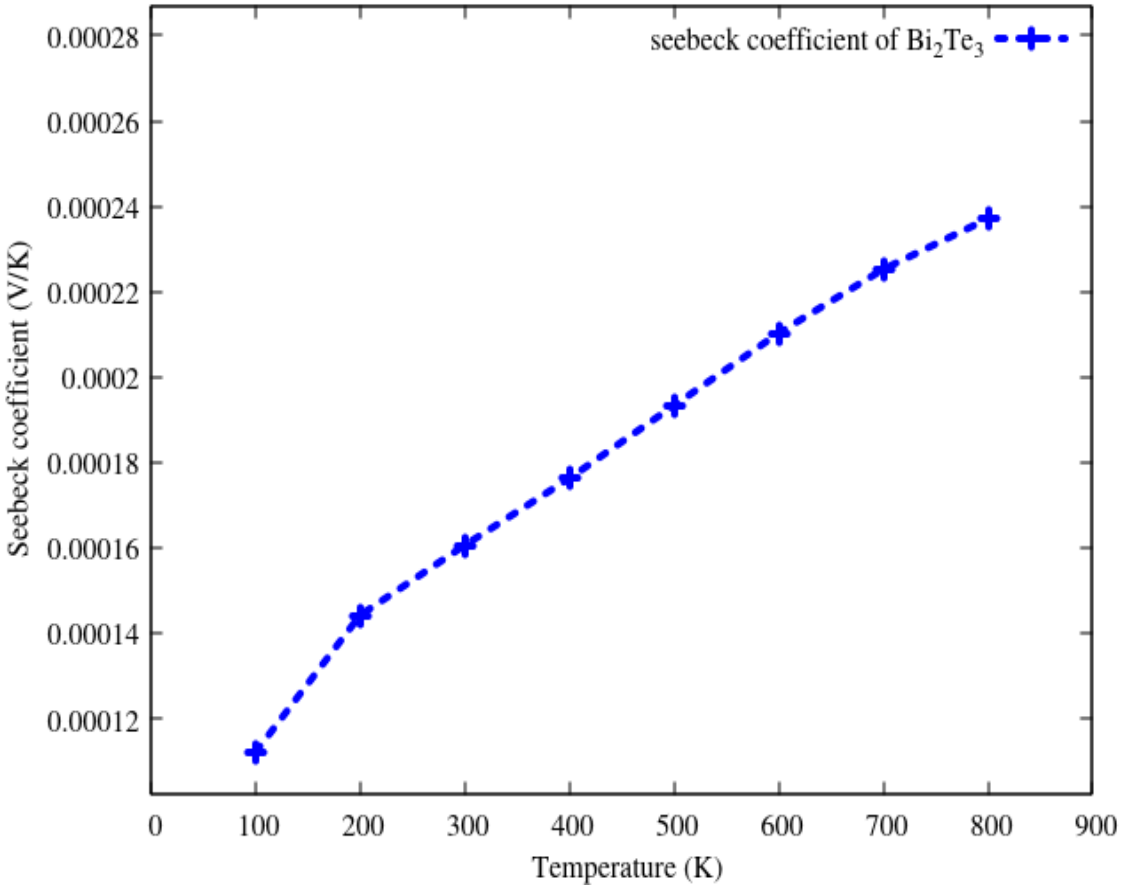

Figure 4.5: Seebeck coefficient of Bi_2Te_3

4.2.5 Power factor (PF) of Bi_2Te_3

The power factor is a fundamental parameter used to evaluate the efficiency of thermoelectric materials. It quantifies the ability of a material to convert temperature differences into electrical power. The power factor is determined by the product of two key properties: electrical conductivity (σ) and the square of the Seebeck coefficient (S^2). Mathematically, the power factor (PF) can be expressed as $PF = \sigma S^2$.

When examining the temperature dependence of the power factor in Bi_2Te_3, it is essential to consider the behavior of electrical conductivity and the Seebeck coefficient. The graph depicting the trend of the power factor with increasing temperature in Bi_2Te_3 (Figure 4.6) reveals an interesting observation: the power factor increases as the temperature rises. The increase in the power factor with temperature can be attributed to the contrasting temperature dependencies of electrical conductivity and the Seebeck coefficient. Firstly, the electrical conductivity of Bi_2Te_3 typically decreases with increasing temperature, as shown

in Figure 4.4. On the other hand, the Seebeck coefficient in Bi_2Te_3 exhibits an opposite trend, increasing with temperature, as demonstrated in Figure 4.5. The interplay between the temperature-dependent changes in electrical conductivity and the Seebeck coefficient leads to the observed increase in the power factor with increasing temperature in Bi_2Te_3. Although the decrease in electrical conductivity would typically lead to a lower power factor, the dominant effect of the increasing Seebeck coefficient exceeds this decline.

This increase in the power factor with temperature is a crucial observation for the performance of Bi_2Te_3 in thermoelectric applications. The power factor is a measure of the combined effect of electrical conductivity and the Seebeck coefficient, and it is directly proportional to the overall thermoelectric figure of merit, which determines the efficiency of thermoelectric energy conversion.

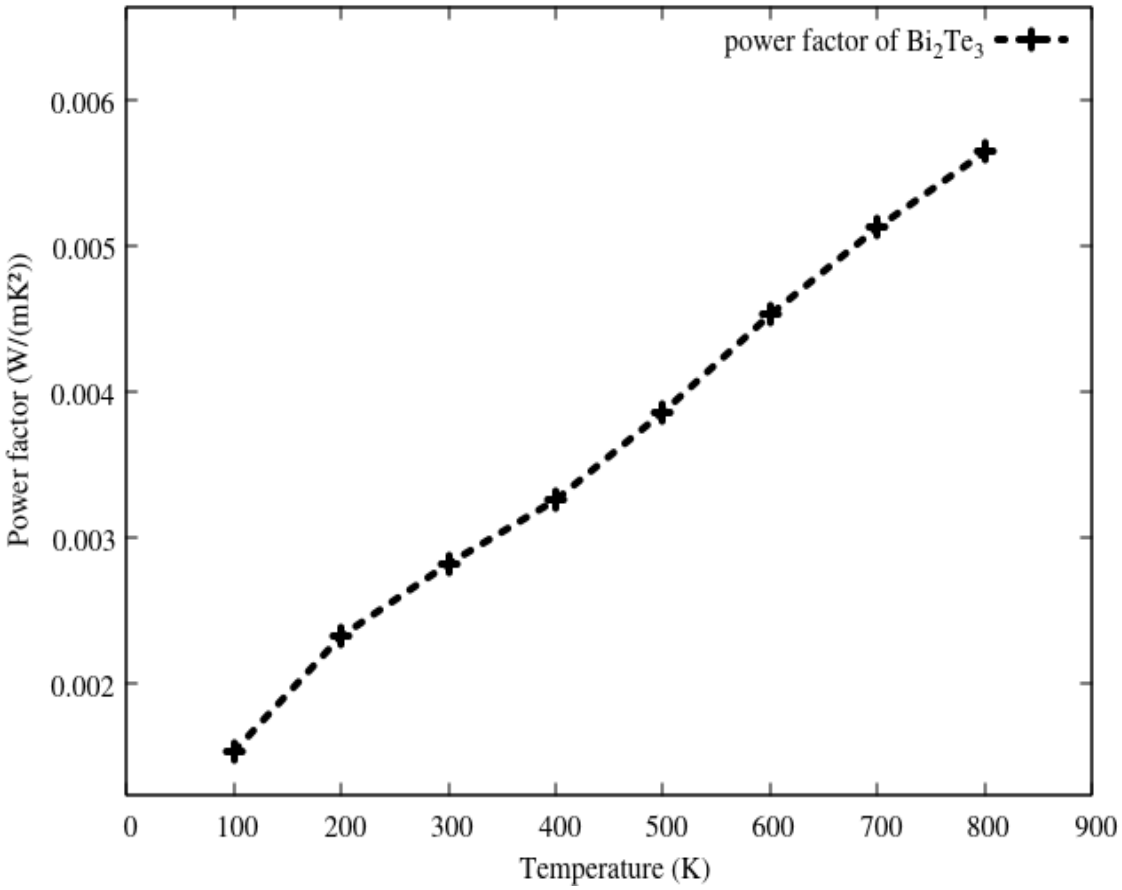

Figure 4.6: Power factor of Bi_2Te_3

Table 4.3: Total thermal conductivity, Power factor and Figure of merit of Bi_2Te_3

Temperature (K)	$\kappa_T(W/mK)$	PF (V/K^2)	ZT
100	2.688	1.52686599E-03	0.05627
200	2.83	2.39225919E-03	0.169
300	2.96	2.84009916E-03	0.3117
400	3.142	3.25894426E-03	0.4136
500	4.1565	3.86033673E-03	0.46434
600	5.2858	4.53193905E-03	0.513
700	6.5825	5.13048377E-03	0.54558
800	7.4944	5.64949168E-03	0.6028

4.2.6 Figure of merit (zT) of Bi_2Te_3

The figure of merit (ZT) of thermoelectric materials is a crucial parameter that quantifies their ability to efficiently convert heat into electrical energy. We have calculated the figure of merit of Bi_2Te_3 by using a dimensionless thermoelectric figure of merit formula described in Equation 2.9 and its results are presented in Table 4.3. The Figure 4.7 show the increseas of the figure of merit (ZT) with increasing temperature in Bismuth telluride (Bi_2Te_3). This behavior can be attributed to the effects of the power factor. The power factor, determined by the product of electrical conductivity (σ) and the square of the Seebeck coefficient (S^2), plays a significant role in determining the figure of merit. As temperature increases, the power factor in Bi_2Te_3 also increases, as observed in the previous discussion. This increase in the power factor with temperature can be attributed to the contrasting temperature dependencies of electrical conductivity and the Seebeck coefficient in Bi_2Te_3. While the electrical conductivity typically decreases with increasing temperature, the Seebeck coefficient exhibits an opposite trend, increasing with temperature. The dominant effect of the increasing Seebeck coefficient exceeds the decline in electrical conductivity, leading to the observed increase in the power factor with increasing temperature. The increment of the power factor with temperature exhibited in Bi_2Te_3 leads to an increasing figure of merit (ZT) with increasing temperature.

The increase in the figure of merit (ZT) of thermoelectric materials, with rising temperature is a key factor for the performance and efficiency of thermoelectric generators. The figure of merit is a key parameter that determines the conversion efficiency of a thermoelectric device in converting heat into usable electrical energy. When the figure of merit increases with temperature, as observed in Figure 4.7, it has significant implications for the performance of thermoelectric generators. Firstly, the improved ZT at higher temperatures directly translates to a higher Carnot efficiency and overall conversion efficiency of the thermoelectric generator. This allows the device to generate more electrical power. Additionally, the rising figure of merit with temperature enables thermoelectric generators to operate effectively over a wider range of temperatures. This expands the applications and versatility of the technology, allowing it to be used in a broader range of heat source conditions. The higher ZT values at elevated temperatures also increase the power density of the thermoelectric generator, meaning more electrical power can be generated per unit volume or mass of the thermoelectric material. In this work, the calculated figure of merit of Bi_2Te_3 was found to be ≈ 0.31 at room temperature (300K), which can be compared with relevant experimental literature data to assess the validity and significance of the computational re-

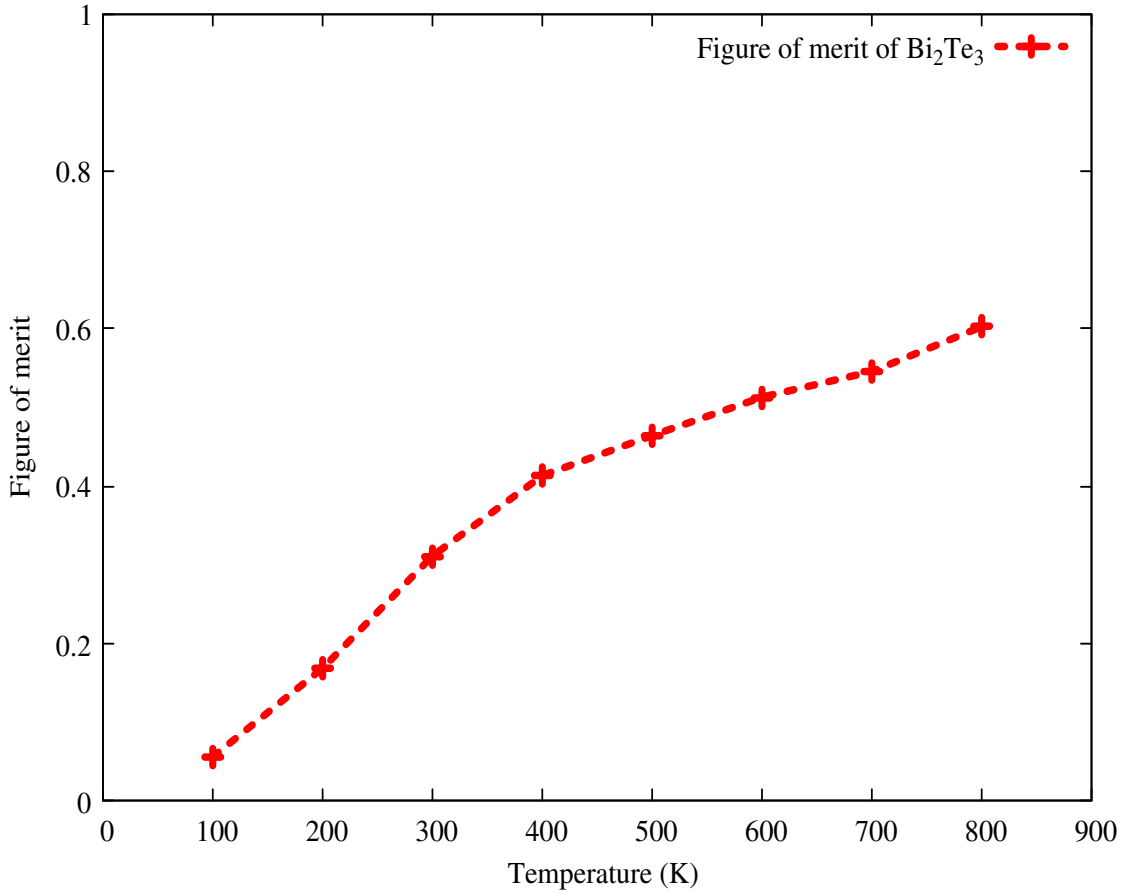

Figure 4.7: Figure of merit of Bi_2Te_3

sults. When comparing the computationally obtained ZT of 0.31 for Bi_2Te_3 at 300K with the literature findings, several relevant studies can be considered. Tu *et al.* (Lv et al., 2020) reported a ZT of 0.3 at 300K for cobalt-doped *BiTeSe* synthesized by the melt method. The close agreement between our result ZT value of 0.31 and the experimental ZT of 0.3 for the cobalt-doped system validates the reliability of the computational approach employed in the present work. This suggests that the theoretical framework and material modeling strategies used can accurately capture the thermoelectric performance of Bi_2Te_3.

Furthermore, the computationally predicted ZT of 0.31 for Bi_2Te_3 is significantly higher than the experimental ZT of 0.22 reported by X. Hu *et al.* (Hu et al., 2019) for Ni-doped Bi_2Se_3 at 300 K. This comparison highlights the superior thermoelectric potential of Bi_2Te_3 compared to the Ni-doped Bi_2Se_3 system. While the computationally obtained ZT of 0.31 is lower than the experimental ZT of 0.6 reported by Nagarjuna *et al.* (Nagarjuna et al., 2020) for fine-grained ball-milled of $Bi_2Te_{2.7}Se_{0.3}$, it is important to note that the latter material was specifically engineered for enhanced thermoelectric performance through advanced techniques such as ball milling and compositional optimization. The computational results in the present work provide a baseline assessment of the thermoelectric potential of pristine Bi_2Te_3, which can serve as a starting point for further optimization through computational technique and targeted experimental investigations. The close agreement between the computationally predicted ZT of 0.31 and the experimental literature values, particularly for the cobalt-doped *BiTeSe* system, validates the reliability and predictive capability of the computational methods employed in this work.

4.3. Efficiency of Thermoelectric generator

Herein, We have calculated the temperature-dependent efficiency of Bi_2Te_3 thermoelectric generator when the hot end's temperature (T_h) varies from 300 to 800 K and the cold end's temperature (T_c) is maintained at 300 K by using the TEG efficiency formula given by:

$$\eta = \frac{T_h - T_c}{T_h} \frac{\sqrt{1+ZT}-1}{\sqrt{1+ZT}+\frac{T_c}{T_h}} \tag{4.1}$$

Where $T = \frac{T_h+T_c}{2}$, T_h and T_c are source and sink temperature, respectively. Z is called a figure of merit of the material used. By substituting all parameters into Eqn 4.1, an approximate efficiency value of Bi_2Te_3 TEG was calculated for temperatures 300, 400, 500, 600, 700, and 800K. The values were found to be η = 0 at 300K, η = 0.02177 at 400K, η = 0.03862 at 500K, η = 0.0526 at 600K, η = 0.0635 at 700K and 0.0756 at 800K as tabulated in table 4.4.

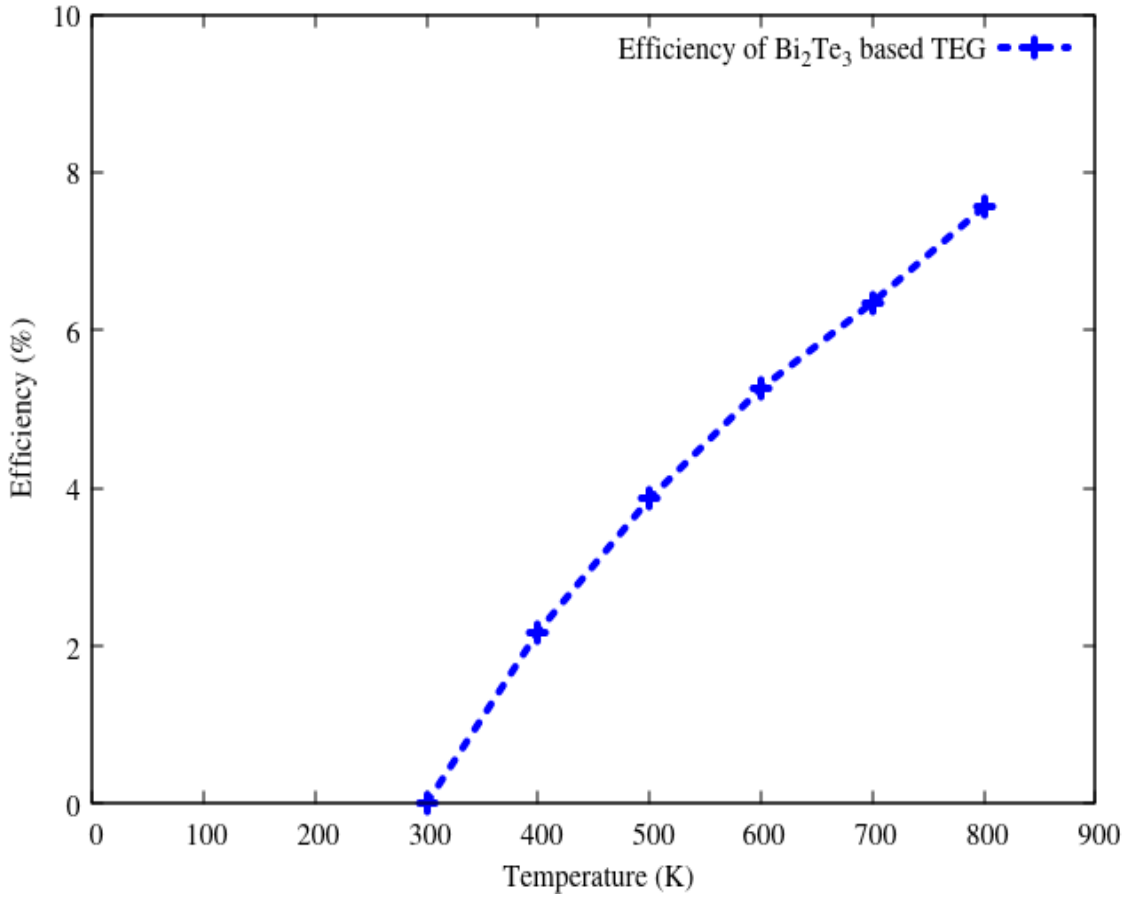

Figure 4.8: Efficiency of Bi_2Te_3 based thermoelectric generator

we examined the relationship between temperature and efficiency of a TEG, as depicted in Figure 4.8. The graph clearly illustrates that the rate of increase in efficiency decreases with higher temperatures. This finding has significant implications for selecting the most economically viable operating temperature range for TEGs. As the temperature increases, the efficiency of the generator also increases; however, the rate of efficiency improvement

Table 4.4: Calculated efficiency of Thermoelectric generator

Temperature (K)	Efficiency (%)
300	0
400	2.177
500	3.862
600	5.26
700	6.35
800	7.56

is slow. At lower temperatures, even slight temperature increments result in substantial efficiency gains. Conversely, as the temperature continues to rise, the efficiency gains become less significant for each subsequent increase in temperature (Figure 4.8). The implications of this observation extend to optimizing the operating temperature range of TEGs. Operating the generator at excessively high temperatures may yield diminishing returns in terms of efficiency improvement. Therefore, it is crucial to identify the temperature range where efficiency gains are most substantial, which ensures both energy conversion efficiency and cost-effectiveness.

The graph can be carefully examined to identify the operating temperature range that is most beneficial. This entails determining the temperature range within which there is an obvious increase in efficiency and choosing a working temperature. As can seen from the graph an obvious rate increase of the efficiency of TEG was observed in a temperature range of 300-600K. This suggests that the identified temperature range of 300-600 K represents the optimal operating temperature for this bismuth telluride-based thermoelectric generator. Within this range, the material properties and the resulting thermoelectric performance are maximized, making it the ideal operating condition and its suitability for various applications that involve waste heat recovery or power generation in this temperature system. Examples may include automotive exhaust heat recovery, industrial process heat utilization, and specialized power generation systems.

In the present study, the calculated efficiency of the Bi_2Te_3-based thermoelectric generator (TEG) was found to be approximately 7.56%. This finding can be compared to the experimental work reported by Ragupathi *et al.* (Ragupathi et al., 2023), who found the efficiency of a similar Bi_2Te_3-based TEG system to be approximately 7.8%. The close alignment between the theoretical efficiency calculated in the current study and the experimentally observed efficiency reported by Ragupathi *et al.* provides strong validation for the reliability and accuracy of the theoretical approach employed in the present Work. The small difference of 0.24 percentage points between the theoretically calculated efficiency of 7.56% and the experimentally observed efficiency of 7.8% reported by Ragupathi *et al*. falls well within the expected margin of error and uncertainty associated with both theoretical modeling and experimental measurements. This close agreement between the theoretical and experimental findings further strengthens the validity and credibility of the present research work, indicating that the theoretical approach employed has successfully captured the essential factors governing the performance of Bi_2Te_3-based TEGs. The theoretical efficiency of 7.56% also approaches the highest experimentally demonstrated value of around 8% for $BiTe$ by Nagarjuna *et al.* (Nagarjuna et al., 2020). This implies that the present theoretical work has made significant strides towards the optimization of Bi_2Te_3 thermoelectric technology, potentially

identifying avenues for further enhancing the performance beyond the current state-of-the-art. Overall, the close alignment between the theoretical efficiency calculated in this study and the highest experimental values reported in the literature validates the rigor and effectiveness of the theoretical approach. This work provides a strong foundation for guiding future experimental efforts and accelerating the development of high-efficiency Bi_2Te_3-based thermoelectric generators for waste heat recovery and other energy conversion applications. The slight variations in efficiency values between the current work and the literature may be attributed to optimization techniques employed in the respective studies. However, the overall agreement in the efficiency range supports the practicality and competitiveness of the thermoelectric generator based on Bi_2Te_3 that is described in this work.

5. CONCLUSION AND RECOMMENDATION

5.1. Summary and Conclusion

This thesis presents a comprehensive investigation into the performance characteristics of a bismuth telluride (Bi_2Te_3) based thermoelectric generator, conducted through rigorous computational simulations. The study employed two complementary methods - non-equilibrium molecular dynamics (NEMD) and Boltzmann transport equation (BTE) - to systematically evaluate the thermoelectric properties of Bi_2Te_3 over a wide temperature range of 100-800K. The NEMD simulations were used to calculate the lattice thermal conductivity, which was found to decrease with increasing temperature due to enhanced phonon scattering. The BTE method was then applied to assess the electronic transport properties, including electronic thermal conductivity, electrical conductivity, and Seebeck coefficient. The results revealed that electronic thermal conductivity increased with temperature, while electrical conductivity decreased, primarily due to the dominant impact of phonon scattering at higher temperatures. Interestingly, the Seebeck coefficient was observed to rise with increasing temperature, as the energy distribution of electrons broadened. By consolidating the computed thermoelectric properties, the dimensionless figure of merit (ZT) was determined, and the efficiency of the Bi_2Te_3-based thermoelectric generator was estimated to be approximately 7.56% when the sink temperature was maintained at 300K and the source temperature was varied from 300-800K, demonstrating good agreement with reported literature values. This comprehensive simulation-based study provides valuable insights into the performance characteristics of Bi_2Te_3 as a promising thermoelectric material, which can inform the design and optimization of advanced thermoelectric energy conversion systems.

5.2. Recommendation

Based on the comprehensive performance evaluation of a Bismuth telluride (Bi_2Te_3) based thermoelectric generator conducted in this thesis, several recommendations can be made. Firstly, the optimization of Bi_2Te_3 composition and microstructure should be explored, as the study has demonstrated the promising thermoelectric properties of Bi_2Te_3. Further refinement of the material could potentially lead to even higher ZT values, thereby enhancing the overall efficiency and performance of Bi_2Te_3-based thermoelectric generators. Secondly, it is recommended to validate the obtained simulation results through carefully designed experimental investigations. While the computational techniques employed in this study, including NEMD and BTE, have shown good agreement with previous experimental work, experimental validation would further strengthen the confidence in the performance potential of Bi_2Te_3 as a thermoelectric material. Additionally, it is suggested to investigate the behavior and performance of Bi_2Te_3 at even higher temperatures, as the study has focused on the performance over a wide temperature range of 100-800K. Exploring the material's performance at even higher temperatures, as thermoelectric generators often operate in high-temperature environments, could potentially expand the application range of Bi_2Te_3-based thermoelectric systems.

Research Fund Acknowledgment

This Research Project is funded by Adama Science and Technology University under the grant number ASTU/SM-R/990/24, Adama, Ethiopia.

References

Allen, P. B., Pickett, W. E., & Krakauer, H. (1988). Anisotropic normal-state transport properties predicted and analyzed for high-t c oxide superconductors. *Physical Review B*, *37*(13), 7482.

Badar, M. S., Shamsi, S., Ahmed, J., & Alam, M. A. (2022). Molecular dynamics simulations: concept, methods, and applications. In *Transdisciplinarity* (pp. 131–151). Springer.

Banoo, K., Lundstrom, M., & Smith, R. K. (2000). Direct solution of the boltzmann transport equation in nanoscale si devices. In *2000 international conference on simulation semiconductor processes and devices (cat. no. 00th8502)* (pp. 50–53).

Bell, L. E. (2008). Cooling, heating, generating power, and recovering waste heat with thermoelectric systems. *Science*, *321*(5895), 1457–1461.

Biswas, K., He, J., Blum, I. D., Wu, C.-I., Hogan, T. P., Seidman, D. N., ... Kanatzidis, M. G. (2012). High-performance bulk thermoelectrics with all-scale hierarchical architectures. *Nature*, *489*(7416), 414–418.

Brownell, E., & Hodes, M. (2014). Optimal design of thermoelectric generators embedded in a thermal resistance network. *IEEE Transactions on Components, Packaging and Manufacturing Technology*, *4*(4), 612–621.

Caballero-Calero, O., Ares, J. R., & Martín-González, M. (2021). Environmentally friendly thermoelectric materials: High performance from inorganic components with low toxicity and abundance in the earth. *Advanced Sustainable Systems*, *5*(11), 2100095.

Cai, Y., Xiao, J., Zhao, W., Tang, X., & Zhang, Q. (2011). A general model for the electric power and energy efficiency of a solar thermoelectric generator. *Journal of electronic materials*, *40*, 1238–1243.

Camacho-Medina, P., Olivares-Robles, M. A., Vargas-Almeida, A., & Solorio-Ordaz, F. (2014). Maximum power of thermally and electrically coupled thermoelectric generators. *Entropy*, *16*(5), 2890–2903.

Cantarero, A., & Àlvarez, F. X. (2014). Thermoelectric effects: Semiclassical and quantum approaches from the boltzmann transport equation. *Nanoscale Thermoelectrics*, 1–39.

Champier, D., Bedecarrats, J.-P., Rivaletto, M., & Strub, F. (2010). Thermoelectric power generation from biomass cook stoves. *Energy*, *35*(2), 935–942.

Chen, D.-L., & Chen, T.-C. (2005). Mechanical properties of au nanowires under uniaxial tension with high strain-rate by molecular dynamics. *Nanotechnology*, *16*(12), 2972.

Cheng, T.-C., Cheng, C.-H., Huang, Z.-Z., & Liao, G.-C. (2011). Development of an energy-saving module via combination of solar cells and thermoelectric coolers for green building applications. *Energy*, *36*(1), 133–140.

Dahlquist, G., & Bjork, A. (1974). Equidistant interpolation and the runge phenomenon. *Numerical Methods*, 101–103.

Ding, L. C., Akbarzadeh, A., & Tan, L. (2018). A review of power generation with thermoelectric system and its alternative with solar ponds. *Renewable and sustainable energy reviews*, *81*, 799–812.

Dong, H., Fan, Z., Shi, L., Harju, A., & Ala-Nissila, T. (2018). Equivalence of the equilibrium and the nonequilibrium molecular dynamics methods for thermal conductivity calculations: From bulk to nanowire silicon. *Physical Review B*, *97*(9), 094305.

Durrant, J. D., & McCammon, J. A. (2011). Molecular dynamics simulations and drug discovery. *BMC biology*, *9*, 1–9.

Enescu, D. (2019). Thermoelectric energy harvesting: basic principles and applications. *Green energy advances*, *1*, 38.

Fairbanks, J. (2008). Thermoelectric applications in vehicles status 2008. *US Department of Energy*.

Gaurav, K., & Pandey, S. K. (2017). Efficiency calculation of a thermoelectric generator for investigating the applicability of various thermoelectric materials. *Journal of renewable and sustainable energy*, *9*(1).

Goldsmid, H. (1956). The thermal conductivity of bismuth telluride. *Proceedings of the Physical Society. Section B*, *69*(2), 203.

Goldsmid, H. J., et al. (2010). *Introduction to thermoelectricity* (Vol. 121). Springer.

Gonzalez-Hernandez, S., & Arias-Hernandez, L.-A. (2019). Thermoelectric thomson relations revisited for a linear energy converter. *Journal of Non-Equilibrium Thermodynamics*, *44*(3), 315–332.

Heremans, J. P., Jovovic, V., Toberer, E. S., Saramat, A., Kurosaki, K., Charoenphakdee, A., ... Snyder, G. J. (2008). Enhancement of thermoelectric efficiency in pbte by distortion of the electronic density of states. *Science*, *321*(5888), 554–557.

Hsu, K. F., Loo, S., Guo, F., Chen, W., Dyck, J. S., Uher, C., ... Kanatzidis, M. G. (2004). Cubic agpb m sbte2+ m: bulk thermoelectric materials with high figure of merit. *Science*, *303*(5659), 818–821.

Hu, X., Xiang, Q., Kong, D., Feng, B., Pan, Z., Liu, P., ... others (2019). The effect of ni/sn doping on the thermoelectric properties of bisbte polycrystalline bulks. *Journal of Solid State Chemistry*, *277*, 175–181.

Huang, B.-L., & Kaviany, M. (2008). Ab initio and molecular dynamics predictions for electron and phonon transport in bismuth telluride. *Physical Review B*, *77*(12), 125209.

Huang, S., & Xu, X. (2017). A regenerative concept for thermoelectric power generation. *Applied Energy*, *185*, 119–125.

Juárez-Huerta, V., Sánchez-Salas, N., & Chimal-Eguia, J. C. (2022). Optimization criteria and efficiency of a thermoelectric generator. *Entropy*, *24*(12), 1812.

Kullmann, W., Eichhorn, G., Rauh, H., Geick, R., Eckold, G., & Steigenberger, U. (1990). Lattice dynamics and phonon dispersion in the narrow gap semiconductor bi2te3 with sandwich structure. *physica status solidi (b)*, *162*(1), 125–140.

Kwan, V., Ballaney, P., Titiksha, & Consta, S. (2023). Limitations of atomistic molecular dynamics to reveal ejection of proteins from charged nanodroplets. *The Journal of Physical Chemistry B*, *127*(21), 4829–4842.

LaGrandeur, J., Crane, D., & Eder, A. (2005). Vehicle fuel economy improvement through thermoelectric waste heat recovery. In *Deer conference* (pp. 1–24).

LeBlanc, S. (2014). Thermoelectric generators: Linking material properties and systems engineering for waste heat recovery applications. *Sustainable Materials and Technologies*, *1*, 26–35.

Lesage, F. J., & Pagé-Potvin, N. (2013). Experimental analysis of peak power output of a thermoelectric liquid-to-liquid generator under an increasing electrical load resistance. *Energy conversion and management*, *66*, 98–105.

Lv, T., Li, Z., Yang, Q., Benton, A., Zheng, H., & Xu, G. (2020). Synergistic regulation of electrical-thermal effect leading to an optimized thermoelectric performance in co doping n-type bi2 (te0. 97se0. 03) 3. *Intermetallics*, *118*, 106683.

Madsen, G. K., Schwarz, K., Blaha, P., & Singh, D. J. (2003). Electronic structure and transport in type-i and type-viii clathrates containing strontium, barium, and europium. *Physical Review B*, *68*(12), 125212.

Mamur, H., & Ahiska, R. (2014). A review: Thermoelectric generators in renewable energy. *International journal of renewable energy research*, *4*(1), 128–136.

Manzano, C. V., Polyakov, M. N., Maiz, J., Aguirre, M. H., Maeder, X., & Martín-González, M. (2019). Pulsed current-voltage electrodeposition of stoichiometric bi2te3 nanowires and their crystallographic characterization by transmission electron backscatter diffraction. *Science and technology of advanced materials*, *20*(1), 1022–1030.

Mary-Rose, M., & Wallenfeldt, J. (2024). Thermoelectric power generator. *Encyclopædia Britannica, Inc.*, 1.

Mili, I., Latelli, H., Charifi, Z., Baaziz, H., & Ghellab, T. (2022). A simple formula for calculating the carrier relaxation time. *Computational Materials Science*, *213*, 111678.

Mori, T., & Maignan, A. (2021). *Thermoelectric materials developments: past, present, and future* (Vol. 22) (No. 1). Taylor & Francis.

Muna, I. I., & Winczewski, S. (2020). Molecular dynamics simulations of thermal conductivity of penta-graphene. *TASK Quarterly*, *24*, 191–220.

Nagarjuna, C., Dharmaiah, P., Kim, K. B., & Hong, S.-J. (2020). Grain refinement to improve thermoelectric and mechanical performance in n-type bi2te2. 7se0. 3 alloys. *Materials Chemistry and Physics*, *256*, 123699.

Nolting, W. (2012). Electronic transport in thermoelectric bismuth telluride.

Očko, M., Žonja, S., & Ivanda, M. (2010). Thermoelectric materials: problems and perspectives. In *The 33rd international convention mipro* (pp. 16–21).

Ouerdane, H., Apertet, Y., Goupil, C., & Lecoeur, P. (2015). Continuity and boundary conditions in thermodynamics: From carnot's efficiency to efficiencies at maximum power. *The European Physical Journal Special Topics*, *224*, 839–864.

Pei, Y., Shi, X., LaLonde, A., Wang, H., Chen, L., & Snyder, G. J. (2011). Convergence of electronic bands for high performance bulk thermoelectrics. *Nature*, *473*(7345), 66–69.

Poudel, B., Hao, Q., Ma, Y., Lan, Y., Minnich, A., Yu, B., ... others (2008). High-thermoelectric performance of nanostructured bismuth antimony telluride bulk alloys. *science*, *320*(5876), 634–638.

Qiu, B., & Ruan, X. (2009). Molecular dynamics simulations of lattice thermal conductivity of bismuth telluride using two-body interatomic potentials. *Physical Review B*, *80*(16), 165203.

Ragupathi, P., Barik, D., et al. (2023). Investigation on the heat-to-power generation efficiency of thermoelectric generators (tegs) by harvesting waste heat from a combustion engine for energy storage. *International Journal of Energy Research*, *2023*.

Rowe, D. M. (2018). *Thermoelectrics handbook: macro to nano*. CRC press.

Ryu, B., Oh, M.-W., Ryu, B., & Oh, M.-W. (2016). Computational simulations of thermoelectric transport properties. *Journal of the Korean Ceramic Society*, *53*(3), 273–281.

Shaikh, F. K., & Zeadally, S. (2016). Energy harvesting in wireless sensor networks: A comprehensive review. *Renewable and Sustainable Energy Reviews*, *55*, 1041–1054.

Sherman, B., Heikes, R. R., & Ure Jr, R. W. (1960). Calculation of efficiency of thermoelectric devices. *Journal of Applied Physics*, *31*(1), 1–16.

Sim, Z. W. (2012). Radio frequency energy harvesting for embedded sensor networks in the natural environment.

Singh, B., Baharin, N. Remeli, M. F., Oberoi, A., Date, A., & Akbarzadeh, A. (2017). Experimental analysis of thermoelectric heat exchanger for power generation from salinity gradient solar pond using low-grade heat. *Journal of Electronic Materials*, *46*, 2854–2859.

Singh, B. S. B. (2023). Thermoelectric generators: Design, operation, and applications. In *New materials and devices for thermoelectric power generation.* IntechOpen.

Singh, J. (2008). *Modern physics for engineers*. John Wiley & Sons.

Snyder, G. J. (2009). Thermoelectric energy harvesting. In *Energy harvesting technologies* (pp. 325–336). Springer.

Snyder, G. J., & Snyder, A. H. (2017). Figure of merit zt of a thermoelectric device defined from materials properties. *Energy & Environmental Science*, *10*(11), 2280–2283.

Snyder, G. J., & Toberer, E. S. (2008). Complex thermoelectric materials. *Nature materials*, *7*(2), 105–114.

Steinhauser, M. O. (2012). Introduction to molecular dynamics simulations: Applications in hard and soft condensed matter physics. *Molecular dynamics-Studies of synthetic and biological macromolecules*, 3–28.

Sun, Y., Liu, Y., Li, R., Li, Y., & Bai, S. (2022). Strategies to improve the thermoelectric figure of merit in thermoelectric functional materials. *Frontiers in Chemistry*, *10*, 865281.

Telkes, M. (1947). The efficiency of thermoelectric generators. i. *Journal of Applied Physics*, *18*(12), 1116–1127.

Termentzidis, K., & Merabia, S. (2012). Molecular dynamics simulations and thermal transport at the nano-scale. *Molecular Dynamics-Theoretical Developments and Applications in Nanotechnology and Energy*, 73–104.

Thacher, E., Helenbrook, B., Karri, M., & Richter, C. J. (2007). Testing of an automobile exhaust thermoelectric generator in a light truck. *Proceedings of the Institution of Mechanical Engineers, Part D: Journal of Automobile Engineering*, *221*(1), 95–107.

Tritt, T. M. (2005). *Thermal conductivity: theory, properties, and applications*. Springer Science & Business Media.

Tundee, S., Srihajong, N., & Charmongkolpradit, S. (2014). Electric power generation from solar pond using combination of thermosyphon and thermoelectric modules. *Energy Procedia*, *48*, 453–463.

Umidbek Turg‘unboy o‘g, X., Islombek Turg‘unboy o‘g, X., Muxammadamin o‘g‘li, M. A., et al. (2024). Prospects in the use of thermoelectric generators for vehicles. *Ta’limning zamonaviy transformatsiyasi*, *6*(1), 62–66.

Verlet, L. (1967). Computer" experiments" on classical fluids. i. thermodynamical properties of lennard-jones molecules. *Physical review*, *159*(1), 98.

Wu, X., Varshney, V., Lee, J., Zhang, T., Wohlwend, J. L., Roy, A. K., & Luo, T. (2016). Hydrogenation of penta-graphene leads to unexpected large improvement in thermal conductivity. *Nano letters*, *16*(6), 3925–3935.

Xiao, J., Yang, T., Li, P., Zhai, P., & Zhang, Q. (2012). Thermal design and management for performance optimization of solar thermoelectric generator. *Applied Energy*, *93*, 33–38.

Yan, R., Xie, W., Balke, B., Chen, G., & Weidenkaff, A. (2020). Realizing p-type nbcosn half-heusler compounds with enhanced thermoelectric performance via sc substitution. *Science and Technology of Advanced Materials*, *21*(1), 122–130.

Yang, W., Zhu, W., Yang, Y., Huang, L., Shi, Y., & Xie, C. (2022). Thermoelectric performance evaluation and optimization in a concentric annular thermoelectric generator under different cooling methods. *Energies*, *15*(6), 2231.

Zebarjadi, M., Esfarjani, K., Dresselhaus, M., Ren, Z., & Chen, G. (2012). Perspectives on thermoelectrics: from fundamentals to device applications. *Energy & Environmental Science*, *5*(1), 5147–5162.

Zevenhoven, R., & Beyene, A. (2011). The relative contribution of waste heat from power plants to global warming. *Energy*, *36*(6), 3754–3762.

Zhang, C., Peng, Z., Li, Z., Yu, L., Khor, K. A., & Xiong, Q. (2015). Controlled growth of bismuth antimony telluride bixsb2- xte3 nanoplatelets and their bulk thermoelectric nanocomposites. *Nano Energy*, *15*, 688–696.

Zhang, X., & Zhao, L.-D. (2015). Thermoelectric materials: Energy conversion between heat and electricity. *Journal of Materiomics*, *1*(2), 92–105.

Zheng, X., Liu, C., Yan, Y., & Wang, Q. (2014). A review of thermoelectrics research–recent developments and potentials for sustainable and renewable energy applications. *Renewable and Sustainable Energy Reviews*, *32*, 486–503.

Appendix

```
# LAMMPS input script for thermal conductivity of bismuth telluride

# thermostatting 2 regions via fix langevin

# Settings

dimension                3

boundary                 p p p

units                    metal

atom_style               atomic

# Variables

variable                 kB equal 0.00008617

variable                 t equal 100

variable                 tlo equal 95

variable                 thi equal 105

# Setup problem

read_data                2x2x2.lammps-data
mass 1                   208.98

mass 2                   127.60

velocity                 all create $t 87287

# Interatomic potential

pair_style               morse 4.5
pair_coeff               1 1 0.085 2.212 4.203

pair_coeff               1 2 0.975 1.285 3.089

pair_coeff               2 2 0.076 1.675 3.642

# Adjusted timestep value
```

```
timestep                0.005

# Heat layers

region                  hot block INF INF INF INF 0 6

region                  cold block INF INF INF INF 20 26

compute                 Thot all temp/region hot

compute                 Tcold all temp/region cold

# 1st equilibration run

fix                     1 all nvt temp $t $t 0.1
thermo                  10

run                     100

velocity                all scale $t
unfix                   1

# 2nd equilibration run

fix                     1 all nve

fix                     hot all langevin $thi $thi 0.1 45623 tally yes

fix                     cold all langevin $tlo $tlo 0.1 78934 tally yes

fix_modify              hot temp Thot

fix_modify              cold temp Tcold

variable                tdiff equal c_Thot - c_Tcold

thermo_style            custom step temp c_Thot c_Tcold f_hot f_cold v_tdiff

thermo                  1000

run                     10000

# Thermal conductivity calculation

compute                 ke all ke/atom

variable                temp atom c_ke/1.5
```

```
print                          "kinetic energy"
fix                             hot all langevin $thi $thi 0.1 45623 tally yes
fix                             cold all langevin $tlo $tlo 0.1 78934 tally yes
fix_modify                      hot temp Thot
fix_modify                      cold temp Tcold
fix                             ave all ave/time 10 100 1000 v_tdif f_ave running
thermo_style                    custom step temp c_Thot c_Tcold f_hot f_cold v_tdiff f_ave
thermo_modify                   lost ignore flush yes
compute                         layers all chunk/atom bin/1d z lower 0.05 units reduced
fix                             2 all ave/chunk 10 100 1000 layers v_temp file profile.langevin
variable                        start_time equal time
# Calculate thermal conductivity
variable                        kappa equal 0.5*(abs(f_hot)+abs(f_cold))/(time-$start_time)*(lx*ly)*(lz)/f_a
run                             20000
print                   "Running average thermal conductivity metal unit style: $(v_kappa:%.5f)"
print                   "Running average thermal conductivity W/mK: $(v_kappa*1.60218e+3:%.5f)"
```